REVIEWS OF TOPICAL PROBLEMS

PACS numbers: 29.40.Wk, **41.60.–m**, 61.80.Fe, **61.85.+p**

Electromagnetic radiative processes in periodic media at high energies

M L Ter-Mikhaelyan

DOI: 10.1070/PU2001v044n06ABEH000886

Contents

1. Introduction 571
2. Diffracted X-ray radiation 573
3. Transition radiation. Resonance transition radiation 574
4. Radiation by uniformly moving particles in more complex structures, DXR+RTR 577
5. Coherent bremsstrahlung and the scope of its applicability 577
6. Radiation effects in channeling (experiment) 581
6.1 High energies; 6.2 Low energies
7. Orientation effects and channeling of charged particles in crystalline matter 585
7.1 Coulomb scattering cross sections; 7.2 Coherence length; 7.3 Coherent scattering in a cubic crystal (orientation effects) and axial channeling
8. Theoretical problems of low-energy radiative electromagnetic processes 589
8.1 Axial and planar channeling; 8.2 Channeling and radiative processes in crystals
9. Theoretical problems of high-energy radiative electromagnetic processes 592
9.1 Introduction; 9.2 Classical theory; 9.3 Constant field approximation
10. Conclusions 594
References 594

Abstract. This review concerns radiative phenomena accompanying the passage of charged relativistic particles and high-energy photons through periodic media. Radiative processes related to the uniform motion or Coulomb scattering of relativistic particles are discussed. The results obtained in this field are widely used in current physical research in such areas as high-energy physics, solid-state physics, technology development, and apparatus design.

1. Introduction

In recent years there has been a growing amount of research on high-energy electromagnetic processes in crystalline and amorphous materials. Most experiments have been carried out at photon frequencies considerably higher than atomic frequencies and with the energies of charged relativistic particles amounting to hundreds of gigaelectronvolts. These problems have been discussed at scientific meetings and workshops all over the world, such as the International Conference on Relativistic Particles in Periodic Media (Tomsk, Russia, 1993 – 1999), the International Workshop on the Radiation Physics of Relativistic Electrons (Tabarz, Germany, 1998), etc. Materials presented at these meetings and used in the present review reflect the state-of-the-art research in the relevant fields of physics as well as the prospects of their future development.

I was first involved in these studies in the 1950s as a post-graduate student at the I E Tamm Theoretical Department, P N Lebedev Physics Institute, USSR Academy of Sciences, guided by E L Feĭnberg. The results obtained before 1970 were summarized in a monograph [1] which is still widely read[1]. I omit here problems pertaining to the study of optical and lower frequencies and refer the interested readers to the well-known reviews of literature, a monograph by V L Ginzburg [2], and the materials of the aforementioned scientific meetings.

The choice of questions to be discussed in what follows is underlain with the basic idea that, at high energies, the length of the particle trajectory along which the processes evolve coherently increases with energy and may reach a macroscopic size. This length is known as the coherence length or formation zone. The history of its discovery and many important applications in high-energy physics is narrated by E L Feĭnberg in his well-known paper and reminiscences of L D Landau [3]. Without going into details of the problem, we note that the coherence length in the bremsstrahlung process generated by a relativistic particle is [1, 3 – 6]

$$L_{\mathrm{coh}} \approx \frac{2E_1 E_2}{\omega m^2 c^3}\,, \tag{1}$$

where E_1 and E_2 are the particle energies before and after the emission, ω is the frequency of the emitted photon, c is the velocity of light, and m is the particle mass.

M L Ter-Mikhaelyan Institute for Physical Research, Armenian Academy of Sciences, 378410 Ashtarak-2, Armenia
Tel. (7-374) 28 81 50. Fax (7-374) 323 11 72
E-mail: mikhael@ipr.sci.am

Received 13 November 2000
Uspekhi Fizicheskikh Nauk **171** (6) 597 – 624 (2001)
Translated by Yu V Morozov; edited by A V Getling

[1] The chapter, paragraph, and formula numbers as well as the remaining text of the English version (excepting a few additions from publications of 1969 – 1972) are identical with those in the Russian edition.

Analogous expressions hold for other radiative processes characterized by manifest directionality at high energies, such as Coulomb scattering, formation of electron – positron pairs, etc. This can be proved by means of calculating the change in the momentum along the direction of motion of the process-initiating particle from the laws of conservation of energy and momentum. It is easy to see that the momentum longitudinally transferred to the medium must decrease with the increase of the energy and directionality of the particles involved in the process. In agreement with the uncertainty principle, this will lengthen the longitudinal distances. If they make a considerable contribution to the process under consideration, the usually employed expressions need to be revised (see Section 7.2 for details).

This observation has been used to study two classes of radiative processes — those involving (1) charged particles subject to Coulomb scattering and (2) particles moving at a constant velocity.

Let us start from considering the former class of processes. The physical idea of such processes was first employed in the studies of Coulomb scattering and interference bremsstrahlung emitted by high-energy electrons in crystals, which L D Landau later suggested to call coherent bremsstrahlung (CB). Those studies were followed by the Landau – Pomeranchuk – Migdal works on the effect of multiple Coulomb scattering on bremsstrahlung in amorphous media (hereinafter referred to as the LPM effect) and by investigations into the influence of the polarization of the medium, which, unlike the well-known Fermi effect, is observed in the direction of particle motion; it is therefore termed the longitudinal density effect, the effect of the polarization of the medium, or simply the TM effect [2]. Today, the longitudinal density effect is also considered in the physics of strong interactions and in quantum chromodynamics (see, for example, Ref. [7] and references therein).

The validity of theoretical considerations was first demonstrated by experiments primarily aimed at studying cosmic rays. Their results are reported in numerous publications cited in Refs [1, 5, 6].

The number of works in this field substantially increased after it was shown [8] that radiative processes in crystals should be considered taking into account the channeling of charged particles and its effects, which had been well known by that time in low-energy nuclear physics [9, 10].

In the present review, the universally adopted term channeling radiation (CR) is used for low-energy particles. For high-energy particles, the acronym CCB is used along with CB to emphasize the importance of channeling, even though CB and CCB are the names of essentially the same process of coherent radiation that takes place during Coulomb interaction with a crystal, which is considered in different approximations.

In parallel to these studies, the second line of research has been conducted, with the objective to elucidate electromagnetic radiative processes initiated by uniformly moving relativistic particles as they pass through inhomogeneous media, including periodic ones. The relationship between these processes and those considered in preceding paragraphs was established in 1972 in Ref. [6].

Resonance (coherent) transition radiation [1] (this term, accepted in the current literature, is abbreviated here to RTR in the further discussion) has been successfully applied to the development of a new class of detectors to be used in an ultrahigh-energy range and also new sources of hard γ-radiation. These works gave incentive to a long series of studies of radiative processes initiated by uniformly moving charged particles in periodic and amorphous media.

Radiation generated in association with X-ray diffraction in crystals is worthy of special note. In what follows, we will use the term diffracted X-ray radiation (DXR) [3]. This is currently the object of many studies aimed at the development of a compact monochromatic X-ray source affording gradual frequency readjustment.

In addition to the common idea linking the processes discussed below, it is necessary to take into account the analogy between light scattering and radiation by charged particles. Electromagnetic wave scattering in heterogeneous media has been studied for many years, and the results obtained ought to be used in radiation research. It may be argued that any light scattering process has its counterpart among the processes of radiation by charged particles. For this reason, in the discussion of radiative processes, we will use the terms adopted in light scattering investigations. To emphasize the analogy between the two sorts of processes in heterogeneous media, we briefly review (see Section 5) the pseudophoton method, which helps one to understand many complicated radiative processes known to proceed at high energies.

The majority of theoretical and experimental studies of radiation processes in crystalline and amorphous materials, starting from the first works, were performed in the 1950s, mainly by Soviet physicists. In order to acquaint the world physical community with the works of Soviet scientists done during the Cold War, the Editorial Board of *Nuovo Cimento* asked several leading physicists to write reviews of their fields of interest. Such reviews were written and published by E L Feĭnberg and, jointly, by E L Feĭnberg and I Ya Pomeranchuk [5]. I was encouraged to write a monograph [1] for the Wiley & Sons Publishing House, which also contributed to the development of these studies in foreign research centers. Nevertheless, the level of theoretical and experimental research in the USSR and former USSR remained much higher than abroad for several decades (until now). Sufficient it to list only reviews published in *Physics – Uspekhi* [2, 5, 11 – 19] and monographs [20 – 31] written at that period by Soviet authors, which actually determined the scientific level of research in the corresponding fields.

Special emphasis should be laid on a series of important studies in high-energy physics which were stimulated by the

[2] The longitudinal density effect was first experimentally discovered by F Arutyunyan and his co-workers at the Institute of Physical Research, Yerevan, Armenia, when they were studying cosmic rays [1]. It was recently confirmed by a large group of physicists in SLAC experiments underway at the Stanford University (Perl M L et al. *Phys. Rev. Lett.* **7** (19) 3550 (1996), see also Ref. [3]). However, no attempts have been made thus far to apply this effect to the development of a new generation of detectors for ultrahigh-energy studies.

[3] Since Section 28 in Ref. [1], where DXR was considered for the first time, was devoted to resonance radiation, the new type of radiation was sometimes also referred to as resonance radiation. Also, it was termed parametric, quasi-Cherenkov, and even polarization radiation. To avoid confusion, we will use the term diffracted X-ray radiation (DXR) throughout this review by virtue of its applicability to both kinematic and dynamic theories. It is in line with the analogous terminology adopted in the theory of light scattering. I am grateful to Professor Nitte, who brought this fact to my notice. It is worthwhile to emphasize that Refs [15, 26] quote publications reporting the results of research carried out in that period and use a similar terminology.

discovery of the fact that, under certain conditions, an ultrarelativistic particle can be devoid of a major part of its field (a 'half-naked' particle). This line of research was pioneered by E L Feĭnberg [13]. Important variables in these studies are the coherence length and the particle's field restoration time ('clothing' time). These studies constitute a self-contained area of high-energy nuclear physics and therefore lie beyond the scope of the present review.

The situation grew more complicated in recent years because novel experimental facilities required theoretical consideration of interference of different forms of radiation and extensive experimental studies which had been suspended in the CIS countries. In contrast, they have been intensified abroad (USA, France, Germany, Japan, Denmark, Belgium, etc.) and very often involve cooperation with physicists of the former USSR.

The present paper describes studies on electromagnetic phenomena in periodic media carried out after the publication of my book [1]. Attempting to review the current state of this problem was motivated by the needs of my physicist colleagues actively working in the field, who encouraged me to revise the monograph [1]. This explains why I sought to preserve in this review the continuity of both the style and notation of the earlier work.

I have actually been divorced from the problem of interest for the last 30 years and will hardly be able to highlight all aspects of its development during this period. I apologize in advance for inevitable flaws and omissions that will be found by specialists; I am prepared to take their notes and suggestions into consideration in subsequent works devoted to similar phenomena in amorphous media.

The review is intended for a wide circle of experimenters and theorists, senior students in physics, and physical engineers who wish to update their knowledge in the rapidly evolving field of high-energy electromagnetic radiation in periodic media. With this in mind, I did my best to avoid a detailed presentation of sophisticated mathematical theories and tried in the first place to concentrate on the physical picture of the phenomena under consideration.

2. Diffracted X-ray radiation

DXR was considered in 1969 and discussed in Chapter 5 (Section 28) of my book [1]. The theoretical description of this phenomenon can be greatly simplified if it parallels the exposition of the theory of X-ray scattering in crystals. By means of expanding the electric field of a fast-moving particle into an integral over time (see Section 5) and the variable part of the dielectric permittivity of the crystal $\varepsilon_1(\mathbf{r})$ into a sum over reciprocal lattice vectors $\mathbf{g}$, we obtain

$$\varepsilon = \varepsilon_0 + \varepsilon_1(\mathbf{r}) ; \qquad \varepsilon_1(\mathbf{r}) = \sum n_{\mathbf{g}} \exp(\mathrm{i}\mathbf{g}\mathbf{r}) , \tag{2}$$

where ε_0 is the constant part of the dielectric permittivity. Further, we use the kinematic theory of X-ray scattering to obtain the following expression for the scattered-field strength at a distance R_0 from the scattering crystal:

$$\mathbf{E}'_\omega(R_0) = \frac{e}{\varepsilon_0 R_0} \sum_{\mathbf{g}} n_{\mathbf{g}} \left[\mathbf{k}' \times \mathbf{k}' \times \left(\frac{\omega \mathbf{v}}{c^2} + \frac{\mathbf{g}}{\varepsilon_0}\right)\right] \times \frac{\delta\left[\omega - (\mathbf{k}' - \mathbf{g})\mathbf{v}\right]}{(\mathbf{k}' - \mathbf{g})^2 - (\omega^2/c^2)\varepsilon_0} . \tag{3}$$

Equation (3) implies a linear polarization of the scattered field. The emission angle can be determined from the condition that the argument of the δ-function vanishes:

$$\cos\theta' = \frac{c}{v\sqrt{\varepsilon_0}} - \frac{(\mathbf{g}\mathbf{v})c}{\omega v\sqrt{\varepsilon_0}} , \tag{4}$$

where θ' is the angle between the particle velocity direction and the direction of motion of an emitted photon with the wave vector $\mathbf{k}'$. The equality (4) is a simple consequence of the laws of conservation of energy and momentum for photon emission by a charged particle in a crystal (see Section 7.2 for more detail). It should be borne in mind that the momentum transferred to the lattice must be quantized so as to be proportional to the Planck constant divided by the crystal lattice period. The equality (4) is also easy to obtain using a formula for the Doppler effect in the case of photon emission by a moving electron. This equality is usually employed in measuring the dependences of the emission angle on the photon energy and on the direction of motion of a charged particle relative to the reciprocal lattice vector.

The energy emitted in a frequency range $\mathrm{d}\omega$ and a solid angle $\mathrm{d}\Omega$ as the path vT is covered at a distance R_0 from the scattering volume is given by the expression

$$\mathrm{d}I_{\omega,\mathbf{n}} = c\sqrt{\varepsilon_0}\,|\mathbf{E}'_\omega|^2 R_0^2 \,\mathrm{d}\omega\,\mathrm{d}\Omega , \tag{5}$$

$$\mathrm{d}I_{\omega,\mathbf{n}} = \frac{e^2\omega^2 T}{2\pi\varepsilon_0^{5/2} c} \sum_g n_g^2 \left|\mathbf{k}' \times \left(\frac{\omega\varepsilon}{c^2}\,\mathbf{v} + \mathbf{g}\right)\right|^2 \times \frac{\delta\left[\omega - (\mathbf{k}' - \mathbf{g})\mathbf{v}\right]}{\left[(\mathbf{k}' - \mathbf{g})^2 - (\omega^2/c^2)\varepsilon_0\right]^2} \,\mathrm{d}\omega\,\mathrm{d}\Omega . \tag{6}$$

Formulas (3) for the polarization, (4) for the angular distribution, and (6) for the radiation energy form the basis of the DXR theory, and their validity has been verified in numerous theoretical and experimental studies.

The first experimental DXR studies were conducted at the Institute of Nuclear Physics, Tomsk [32, 33]. They were followed by experiments in Yerevan [34] and then in Kharkov [35]. Ref. [36] reported for the first time DXR induced by protons. It was shown in Refs [37–39] that the results of experiments obtained by that time could be explained fairly well in the framework of the kinematic theory of DXR [4]. A quantum theory of DXR was developed in Ref. [40], which also demonstrated that this theory transforms into the classical theory described in Ref. [1] if the recoil of the emitted photon is neglected. It is worthwhile to note that the dynamic theory of DXR was developed by analogy to the dynamic theory of X-ray scattering and described in a textbook [26] and in monographs [24, 23].

Numerous experimental studies carried out over recent years have further extended our knowledge of DXR. Major characteristics of DXR (monochromatism with a possibility to gradually readjust the frequency, the direction of emission readily distinguishable from the direction of motion of the emitting particle, the narrow energy and angular distribution of radiation, and finally the small size of the experimental unit) indicate that it may be an important source of X-ray radiation in the future.

A series of joint studies [41, 42] have recently been completed by a group of physicists of Darmstadt, Kharkov, Rossendorf, and Johannesburg at the superconducting

[4] At the International Workshop on Radiation Physics (Tabarz, Germany), V I Baryshevskiĭ pointed out that the dynamic theory of DXR is needed to explain the results of the experiment reported in Ref. [53].

S-DALINAC facility at the Institute of Nuclear Physics, Darmstadt, which operates at electron energies below 10 MeV. The DXR line width was measured with an absorption technique, using a copper foil. The DXR peak was scanned along the K-edge of the absorption line of copper atoms. The experimentally determined spectral density of peak emission was $I = 0.95 \times 10^{-7}$ photons (electron sr eV)$^{-1}$, and the measured line width was 48 eV. Figure 1 borrowed from Ref. [41] shows the DXR spectrum near the line of energy 9 keV obtained upon the irradiation of a 55 μm diamond monocrystal by electrons with an energy of 6.8 MeV. The crystal was placed in a goniometer parallel to the (111) crystallographic plane and perpendicular to the plane containing **p** and the radiation direction θ'. By means of changing the tilt angle ϕ, it was possible to modulate the energy of the emitted photon, in accordance with formula (5). The angular divergence of the electron beam was less than 3 mrad, the energy dispersion 40 keV, and the spot size on the crystal ~ 1 mm. The authors argue that, upon taking into account all line broadening effects (multiple scattering, geometric size of the detector), the line width must be of the order of 1 eV. They managed for the first time to achieve a DXR intensity of $\sim 10^{-7}$ photons (electron sr eV)$^{-1}$.

In Refs [43, 44], the DXR line widths were determined to be 1.2 and 3.5 eV in a silicon crystal for the case of photon reflection from the (111) and (022) planes at photon energies of 4966 and 8332 eV. Measurements of DXR line widths now underway at the MAMI microtron in Mainz are expected to yield the relative width $\Delta E/E = 10^{-5}$ upon the reflection from the (333) plane in a silicon crystal. DXR spectral and angular characteristics determined over a wide energy range (from several megaelectronvolts to a few gigaelectronvolts) are consistent with theory [1].

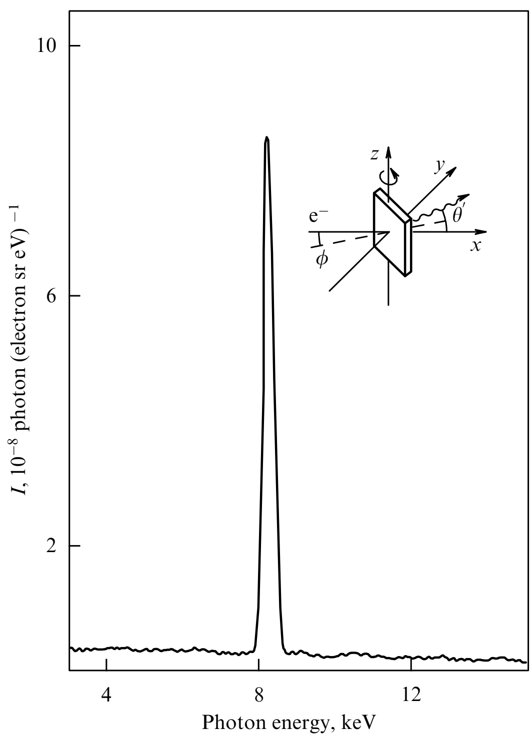

Figure 1. Spectrum of DXR emitted by 6.8 MeV electrons at an observation angle of $\theta' = 42.9°$ to the electron velocity direction. The insert illustrates the possibility to modulate the photon energy by changing the tilt angle ϕ [41].

The results of the most recent experiments reported by German physicists (W Heisenberg Institute, Munich, and Institute of Nuclear Physics, Darmstadt) [46, 47] demonstrated a 100% polarization of DXR, in agreement with theory [1]. These investigators for the first time used a polarimeter in which a new method was employed based on the orientational dependence of photoeffect on DXR polarization [47]. This makes it possible to develop a universal detector operating in the X-ray range, for spectroscopy, polarimetry, and image formation.

The distribution of photon polarization directions of DXR as a function of the emission angle, recently estimated in Ref. [48] from theory [1], is consistent with the experimental and calculated values obtained in Refs [45, 46] for DXR emitted into the forward and backward hemispheres. However, the calculations in Ref. [48] are at variance with those in Refs [45, 46] for radiation at right angles. This may be due to the neglect of the density effect [49] in Refs [45,46] (A Shchagin, private communication). The discrepancy between theoretical calculations [45, 46, 48] and experimental data on forward-directed radiation [50] remains to be resolved in further studies (R Kottaus, private communication).

In conclusion of this brief review of DXR, it is worthwhile to note that there is still no clear understanding of many more complicated theoretical and experimental problems. In particular, this pertains to the scope of applicability of the kinematic and dynamic DXR theories and the relationship between the latter theory and experimental findings [51 – 53]. Ref. [54] takes into consideration effects of multiple scattering and photon absorption on DXR; however, they need a more careful inspection. Effects of temperature, inhomogeneity, acoustic waves, and other factors are poorly known although they are considered in a number of publications (see Refs [55, 56] and the literature cited therein). Ref. [55] deals with the effect of the crystal temperature on DXR and shows that the introduction of the Debye – Waller thermal factor, natural in such cases, makes it possible to explain the experimental findings. It is worthwhile to mention here an experiment [56], so far unique, designed to evaluate ultrasound and temperature gradient effects on DXR. It has demonstrated a rise in the DXR intensity under the influence of these factors. The authors of Ref. [56] believe that this experimental result can be attributed to the bending of crystal lattice planes.

Nevertheless, the DXR intensity reached thus far in the kiloelectronvolt range is of the same order as the intensity of synchrotron radiation in large cyclic accelerators. It is important that the facilities used to study DXR are simple and compact [57]. Some recent publications deal with different forms of radiation, e.g. DXR and RTR, DXR and CB or DXR and CR. They will be considered in greater detail in Sections 4 and 6.2. Also, I believe in the importance of a consistent theoretical consideration of DXR, with calculations taking into account channeling effects. Moreover, it is paramount to evaluate the limits of applicability of the kinematic theory and the necessity to use the dynamic theory of DXR [23, 24, 26] in on-going experiments.

3. Transition radiation. Resonance transition radiation

The Ginzburg – Frank (GF) transition radiation (TR) discovered in 1944 came to be the center of physicists' attention after the expression for the TR intensity derived by these investigators became a subject of study in the X-ray range in 1959. At that time, the works concerning the longitudinal density effect in bremsstrahlung [49] and in the coherence length [1, 3, 4] were already widely known. This greatly facilitated the extrapolation of the results of these studies to transition radiation [58–60].

However, the intensity of transition radiation emitted by a particle as it intersects a single interface between two media is low. It was proposed to enhance it using media composed of many plates [60], i.e. periodic media [61]. This implied the necessity of taking into account that a particle traveling in an arbitrary periodic medium is able to emit only the frequencies that are (for nonrelativistic particles) multiples of the frequency of traversing the period of the medium. At arbitrary energies, this condition (it will hereinafter be referred to as the resonance condition and the corresponding radiation as the resonance transition radiation, or RTR) is somewhat more complicated and assumes the form [61, 62]

$$\cos\theta' = \frac{c}{v\sqrt{\varepsilon_0}} - \frac{2\pi rc}{l\omega\sqrt{\varepsilon_0}}\cos\theta\,, \tag{7}$$

where ω is the radiation frequency, v is the velocity of the emitting particle, ε_0 is the dielectric permittivity of the medium [defined for a periodic medium below; see (8)], θ' is the photon emission angle measured from the particle's velocity direction, θ is the angle of entrance of the particle into the one-dimensional periodic medium, l is the period of the medium, and r is the number of the emitting harmonic.

RTR consists of radiation due to a number of overlapping harmonics, each of them being characterized by a specific radiation threshold determined by the emitting particle energy and the parameters of the medium. The resonance condition (7) is easy to obtain using the Doppler formula or from the energy and momentum conservation laws, provided that only quantized momentum can be transferred to the periodic medium. The theory of RTR was set forth in detail in Ref. [1] and has not undergone substantial modifications by now.

A layered medium composed of a large number of periodically arranged isolated plates (Fig. 2a) proved to be most convenient for experimental studies. For a layered medium, $\sqrt{\varepsilon_0}$ in (7) has the simple form

$$\sqrt{\varepsilon_0} = \frac{l_1\sqrt{\varepsilon_1} + l_2\sqrt{\varepsilon_2}}{l_1 + l_2}\,, \tag{8}$$

where l_1 and l_2 are the plate thicknesses and ε_1 and ε_2 are their dielectric constants.

For frequencies much higher than atomic ones, the condition $\cos\theta' \leqslant 1$ entails conditions on the maximum and minimum radiation frequencies for any harmonic:

$$\omega_{\max} = \frac{4\pi cr}{l}\left(\frac{E}{mc^2}\right)^2 \geqslant \omega \geqslant \frac{l\omega_0^2}{4\pi cr} = \omega_{\min}\,. \tag{9}$$

Here, ω_0 is the plasma frequency:

$$\omega_0^2 = \frac{4\pi NZe^2}{m_e}\,, \tag{10}$$

where, for a layered medium,

$$NZ = \frac{N_1Z_1l_1 + N_2Z_2l_2}{l}\,, \qquad l = l_1 + l_2\,. \tag{11}$$

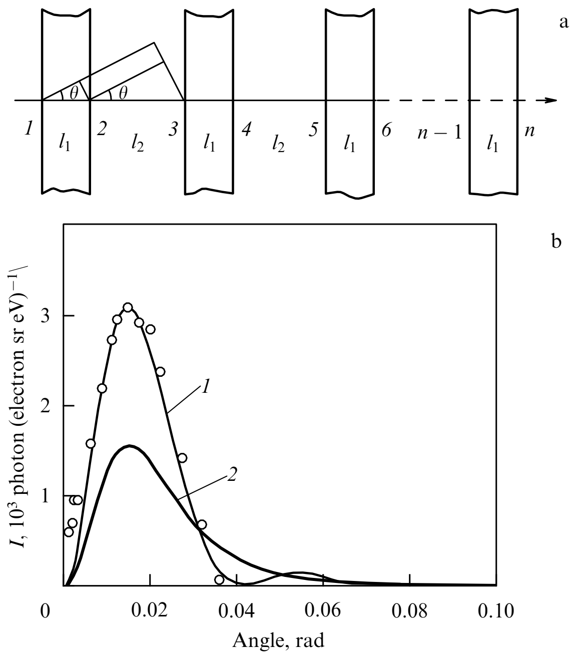

Figure 2. (a) Layered medium. (b) First observation of TR in the keV range: (*1*) angular TR distribution for coherent summation at a 1 μm beryllium plate (good agreement between theory and experiment) and (*2*) computed angular TR distribution for incoherent summation of TR from the two plate surfaces [70].

An expression for the threshold particle energy for the emission of the rth harmonic follows from inequality (9). The radiation intensity in a layered medium is determined by the following formula (see formula (28.92′) in Ref. [1], or [62]):

$$\mathrm{d}I_{\omega,\theta} = \frac{e^2\theta^3\,\mathrm{d}\theta\,\mathrm{d}\omega}{2\pi c} \times \left|\frac{\varepsilon_2-\varepsilon_1}{\left[1-(v/c)\sqrt{\varepsilon_1}\cos\theta\right]\left[1-(v/c)\sqrt{\varepsilon_2}\cos\theta\right]}\right|^2 \times \sin^2\left[\frac{l_1\omega}{2c}\left(1-\frac{v}{c}\sqrt{\varepsilon_1}\cos\theta\right)\right]\frac{\sin^2(n\beta/2)}{\sin^2\beta}\,, \tag{12}$$

where the first multiplier corresponds to the transition radiation at one interface, i.e. GF radiation, the second one determines the interference of radiation from the two plate surfaces, and the third corresponds to the coherent summation of radiation from all plates. The quantity

$$\beta = \left(1-\frac{v}{c}\sqrt{\varepsilon_1}\cos\theta\right)\frac{\omega l_1}{2v} + \left(1-\frac{v}{c}\sqrt{\varepsilon_2}\cos\theta\right)\frac{\omega l_2}{2v}\,. \tag{13}$$

At a sufficiently large number of plates, the last multiplier in (12) can be replaced by a δ function which specifies the resonance condition (7). Of importance in the RTR theory is the coherence length that we introduced in [1] (see formulas (28.3)–(28.13) in Ref. [1] or Section 7.1). For example, independent summation of radiation from individual plates takes place if the distances between them exceed the coherence length; in this case, the radiation energy is proportional to the energy of the emitting particle. In an opposite situation, interference phenomena must be taken into account. The RTR spectrum will be concentrated near the minimum radiation frequencies (see Fig. 58a, b in Ref. [1]), and the emitted energy will tend to saturation. Naturally, similar events will take place in other periodic media. Effects of absorption, diffuse interfaces, and multiple scattering are considered in Ref. [62] and summarized in Ref. [1].

The results of experimental RTR studies carried out before 1970 are presented in detail in Ref. [1]. Pioneering experimental studies of RTR were conducted and a new type of detector for high-energy charged particles was developed by F R Arutyunyan, K A Ispiryan, and A G Oganesyan in 1963 [63] (see also Refs [64 – 66]). The sensitivity of RTR detectors (RTRD) was further improved at a later time (see, for instance, Refs [67 – 69] containing references to publications that appeared after 1969).

Among the experimental studies performed after the monograph [1] was published, Ref. [68] deserves particular mention, since it provides highly accurate measurements of RTR spectra, which definitively confirm theoretical predictions. The same refers to Refs [6, 64, 65] reporting TR studies in porous materials for which the resonance condition can be neglected.

Today, large accelerators at CERN, the E Fermi National Accelerator Laboratory, the DESY laboratory, and other research centers are equipped with RTR detectors to identify high-energy particles. It should be emphasized that RTR detectors ought to be employed only in an ultrarelativistic energy range where Cherenkov detectors measuring particle velocities are inapplicable. RTR detectors identify particles according to the number of photons they emit in a periodic medium, whose energies normally lie in a kiloelectronvolt range. Since the RTR intensity is low (approximately one photon per 100 particles intersecting one interface between two media), and about 100 optical photons per 1 cm path are emitted in the form of Vavilov – Cherenkov radiation, it is evidently senseless to use RTR detectors in the range within which Cherenkov detectors are applicable.

A new impetus was given to RTR research in 1985 by the possibility to use RTR in another area of radiation physics. It turned out that it can serve as a new source of adjustable coherent radiation in a kiloelectronvolt range.

The first experiments were made jointly by two groups of physicists, from the Stanford University (R H Pantell and co-workers) and E O Lawrence Livermore National Laboratory (B L Berman and co-workers) (see Refs [70, 71] and references therein). In their studies, a linear particle accelerator supplied 17.2, 25, and 54 MeV beams, which penetrated a stack of 18 foils, each 1 μm thick. The stacks were made of beryllium, carbon, aluminium or mylar foils. The interfoil separation was 0.75 mm (carbon-foil stack) or 1.5 mm (beryllium and aluminium-foil stacks). The RTR angular distribution and intensity values obtained in these experiments agree with the above theoretical data. The investigators concluded that an intense, monochromatic, easily tunable, forward-directed, polarized X-ray source can be a promising tool for submicron lithography. Indeed, they subsequently managed to obtain a lithograph with a resolution of 0.5 μm [72]. However, no interference effects of radiation from different beryllium foils were observed [70, 71] (Fig. 2b), although in Ref. [73] the same authors noted an unusual interference pattern.

Joint studies of Belgian and French physicists at the Accelerateur Lineaire de Saclay (ALS) also brought about interesting data on interference effects in RTR [75] (Fig. 3). The same group obtained a lithograph with a resolution of

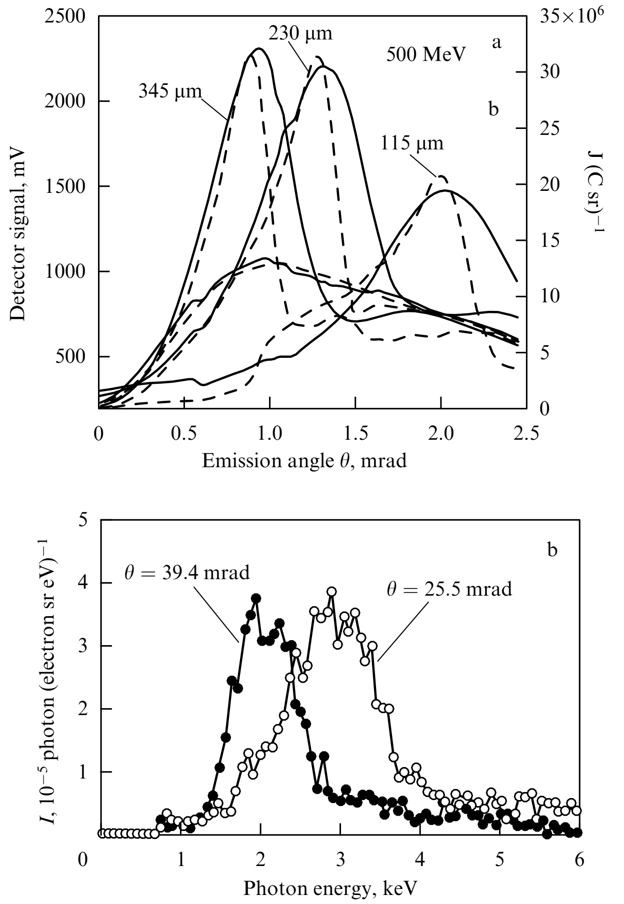

Figure 3. (a) Angular distribution of RTR emitted from a stack of 8 mylar foils of thickness $l_1 = 3.8$ μm. Solid lines: experiment; dashed lines: theory. Lower curves: theory and experiment at $l_2 = 1.5$ mm, before interfoil coherence effects become apparent, and at $l_2 = 345$, 230, and 115 μm,with pronounced coherent effects due to the summation of radiation from different foils [74, 75]. (b) Dependence of radiation intensity on the emitted photon energy for two angles of entrance to a periodic medium (observation of the first-harmonic RTR).

0.3 μm. The authors of Ref. [76] observed the spatial distribution of RTR in a soft spectral region (1 – 3 keV) at electron energies of 50 – 228 MeV. They noted that RTR was emitted throughout the multifoil radiator stack (which served as a periodic medium) and concentrated within a cone the angle of which increased with increasing electron energy. A change of parameters (electron energy or the size of the structures forming the periodic medium) resulted in a decreased intensity of interference and in the emission of TR for which the radiation angle was inversely proportional to the electron energy, in compliance with the TR theory (Fig. 4).

A large series of RTR research was performed by physicists from the universities of Kyoto, Tohoku, Hiroshima (Awata, Tanaka et al.), and Tokyo (Endo et al.) and from the physical laboratories of the Japanese corporations Nippon and Toshiba (Yamada et al.) [77 – 80]. The studies at the accelerator in Tokyo with an electron energy of 1 GeV [78] were carried out in cooperation with the Tomsk Institute of Nuclear Physics (A P Potylitsyn). Their results are in good agreement with the RTR theory.

Another series of studies concerned low-energy electrons. The primary objective of this work was not only to study resonance processes in RTR but also to choose optimal

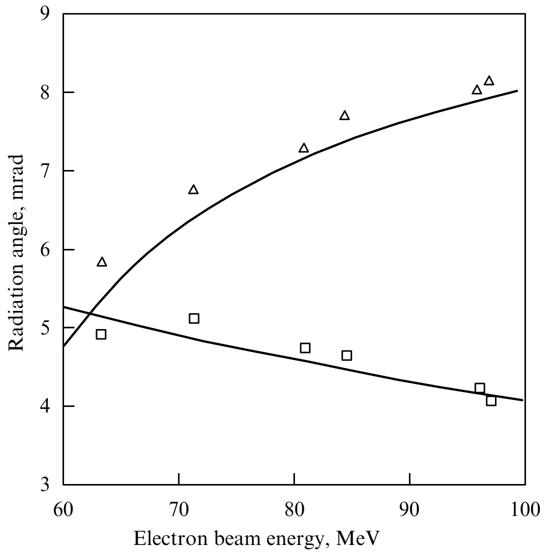

Figure 4. Dependence of the emission angle at the peak intensity on the particle energy for incoherent TR (□) and coherent RTR (△). Solid lines: calculated TR and RTR [76].

parameters of the electron beam and medium characteristics for different applications of RTR. These studies are of great practical and scientific value for the development of RTR theory and for the construction of new radiation sources emitting in a kiloelectronvolt range.

Periodic media composed of plates a few hundred nanometers thick were used for the first time in Ref. [79]. This enabled the authors to distinguish the first-harmonic radiation in the RTR spectrum within a photon energy region of 2–4 keV and to determine the peak position depending on the observation angle. The layered medium consisted of alternating plates of nickel ($l_1 = 176$ nm, radiator) and carbon ($l_2 = 221$ nm). The electron energy was 15 MeV. The results are shown in Fig. 3b. The authors maintain that the intensity of RTR achieved in their experiment exceeds that of synchrotron radiation in the existing particle accelerators. Theoretical aspects of RTR in such media were considered in Ref. [81].

4. Radiation by uniformly moving particles in more complex structures, DXR + RTR

It was understood in the 1990s that DXR and RTR intensities need to be increased if efficient sources of radiation in a kiloelectronvolt range are to be created. Accordingly, more complex, combined periodic media were proposed [82]. Studies in this area were initiated and are carried out jointly by Japanese and Russian physicists.

Targets made of three 16 μm thick crystals were bombarded by 800 MeV electrons at the Tomsk synchrotron and by 900 MeV electrons at the Tokyo linear accelerator [83]. This was expected to lead to a significant rise in the radiation intensity because the very first crystal produced RTR, in addition to DXR, which underwent Bragg diffraction on the second crystal. It is worthwhile to note that the RTR intensity and spectral width are much larger than the respective DXR characteristics, while the angular widths of the two radiation forms are of the same order of magnitude. The difference in the angular distribution consists in that RTR is directed along the electron velocity and DXR along the Bragg angles of reflection from the corresponding planes of the crystal reciprocal lattice. In the above experiments, a 1.7-fold enhancement of radiation was achieved. The authors of Ref. [83] proposed the acronym PRTR for the new class of radiation, which we substitute by DRTR (diffracted RTR) to maintain the uniformity of style in this paper. This abbreviation will be used throughout the remaining text.

These studies were continued by a group of investigators using an electron beam of 900 MeV to bombard a target composed of 10 mylar films and a graphite crystal [84]. According to the authors, the intensity of DRTR directed at the Bragg angles is significantly higher than that of RTR, even with a small number of films.

The most recent joint study of this series [85] was designed to characterize radiation in a kiloelectronvolt range emitted from a target exposed to 900 MeV electrons. The target consisted of 1–100 monocrystalline silicon plates 16 μm thick each. The DRTR intensity of photons with an energy of 35.5 keV turned out to be comparable with the intensity of synchrotron radiation emitted by 1.7 GeV electrons in a storage ring. The investigators also examined the dependence of the radiation intensity on the number of plates in the target, which had been discussed in an earlier paper [81].

References [85, 86] and also [91] (presented at a Workshop in Tabarz, Germany, 1998) provided a theoretical substantiation of the relationship between RTR and the diffracted radiation emitted as a charged particle passed parallel to a surface with periodic inhomogeneities. In these experiments, a beam of electrons was sent over a crystal plate of gallium arsenide which had periodic inhomogeneities at the surface in the form of 300 strips 10 μm in width and 100 μm in height lying 33 μm apart. The experimenters observed composite DXR and DRTR radiation, with the intensity of the latter being much higher than that of the former.

A large number of theoretical studies have recently been devoted to the interference of different forms of radiation. A method for the separation of DXR and DRTR was proposed in Ref. [87]. Ref. [88] shows that the DXR output in a mosaic crystal does not significantly differ from that in an ideal one, while the output of DRTR is considerably higher. Ref. [89] presents a theoretical consideration of TR diffraction in a crystalline structure. A number of theoretical works have been published in the proceedings of recent international workshops [90, 91]. Sections 5 and 6.2 of this review will be devoted to combinations of DXR and RTR with other types of radiation, in particular, with CB and CR.

5. Coherent bremsstrahlung and the scope of its applicability

It has been mentioned above that CB was the first effect for which the introduction of the coherence length proved crucial and led to a radical revision of the then prevailing theory of bremsstrahlung in crystalline media. Following the extensive studies of the 1950s–1970s, which provided experimental data in support of virtually all theoretical premises, CB began to be used in the world's leading laboratories to obtain monochromatic and polarized photon beams. This greatly promoted the further development of experimental physics. The results of research obtained in that period are comprehensively presented in Ref. [1] together with all necessary references to experimental and theoretical studies published before 1970. It remains to be noted that at recent international workshops [90, 91] N Nasonov reported the interference of

CB and DXR and the suppression of the density effect [49] in thin crystal layers.

The easiest way to present the CB theory is to allude to the method suggested by Fermi, Weizsaecker, and Williams and known in the literature as the equivalent-photon, or pseudophoton method. With the aid of this method, it is easy to calculate the probabilities of various radiative processes. We present here a short list of expressions necessary to consider a large number of radiative processes.

The electric field created by a particle with a charge Ze in uniform motion along the x axis with a speed v is, at a point with the coordinate $\mathbf{r}(x = vt, \rho)$ (Fig. 5),

$$E_{\parallel} = \gamma \, \frac{Zevt}{(\rho^2 + v^2 t^2 \gamma^2)^{3/2}} \, , \qquad E_{\perp} = \gamma \, \frac{Ze\rho}{(\rho^2 + v^2 t^2 \gamma^2)^{3/2}} \, , \tag{14}$$

where

$$\gamma = \frac{1}{\sqrt{1-\beta^2}} \, , \qquad \beta = \frac{v}{c} \, . \tag{15}$$

The magnetic-field vector lies in the plane perpendicular to the velocity direction and the electric field vector and is defined by the expression

$$\mathbf{H} = \frac{1}{c} \, [\mathbf{vE}] \, . \tag{16}$$

The electromagnetic field at the point $\mathbf{r}(vt, \rho)$ is concentrated in the interval of time

$$t_{\text{eff}} \approx \frac{\rho}{v\gamma} \, , \tag{17}$$

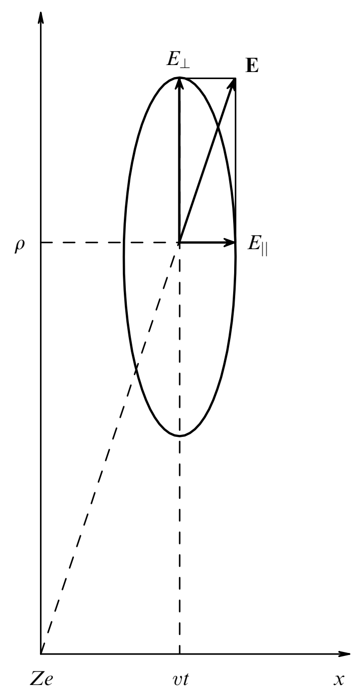

Figure 5. Electric field of a relativistic particle in motion along the x axis at point $\mathbf{r}(vt, \rho)$; $E_{\parallel}$ and $E_{\perp}$ are the field components parallel and perpendicular to the direction of particle motion. If we place the charge Ze at the center of the ellipse and direct radius vectors from the center to their points of intersection with the ellipse, then we will obtain an illustration of the field of a fast-moving charge in the form of a 'pancake'.

with $E_{\perp} \gg E_{\parallel}$. Thus, the electromagnetic field created by a relativistic particle resembles a pancake compressed in the velocity direction, with the electric and magnetic fields perpendicular to the direction of motion. The electromagnetic field has a linear polarization. The Fourier transform of the electric-field vector $E_{\perp}$ with respect to time gives

$$E_{\omega} = \gamma \, \frac{Ze\rho}{2\pi} \int_{-\infty}^{+\infty} \frac{\exp(-\mathrm{i}\omega t) \, \mathrm{d}t}{(\rho^2 + v^2 t^2 \gamma^2)^{3/2}} \, . \tag{18}$$

At frequencies

$$\omega \ll \omega_{\max} = \frac{v\gamma}{\rho} \, , \tag{19}$$

we have

$$E_{\omega} = \frac{Ze}{\pi v \rho} \, . \tag{20}$$

For frequencies in excess of $\omega_{\max}$, the field strength E_{ω} falls sharply. The Pointing vector is

$$S_{\omega\rho} = cE_{\omega}^2 = \frac{Z^2 e^2 c}{\pi^2 v^2 \rho^2} \, . \tag{21}$$

In order to obtain the total energy flux, Eqn (21) must be integrated over the impact parameter ρ:

$$S_{\omega} \, \mathrm{d}\omega = \frac{2Z^2 e^2 c}{\pi v^2} \ln \frac{\rho_{\max}}{\rho_{\min}} \, \mathrm{d}\omega \, . \tag{22}$$

Hence, the action of a fast-moving particle is equivalent to that of a photon flux

$$n_{\omega} \, \mathrm{d}\omega = \frac{S_{\omega}}{\hbar\omega} \, \mathrm{d}\omega = \frac{2Z^2 e^2 c}{\pi \hbar v^2} \, \frac{\mathrm{d}\omega}{\omega} \ln \frac{\rho_{\max}}{\rho_{\min}} \, . \tag{23}$$

The values of the parameters $\rho_{\max}$ and $\rho_{\min}$ depend on the specific situation. Therefore, an arbitrary process induced by a photon with a cross section $\sigma(\omega)$ corresponds to the process initiated by a particle with the cross section

$$\sigma_{\text{part}} = \int n_{\omega} \sigma(\omega) \, \mathrm{d}\omega \, . \tag{24}$$

For the study of the angular distribution and polarization properties of radiation, expression (24) needs to be modified by including the dependence on angular variables, photon polarizations, and spin properties of the particles in the cross section $\sigma(\omega)$ and in n_{ω}. Then, the probabilities of coherent bremsstrahlung and pair formation (see Section 3 in Ref. [1]) can be obtained without serious difficulty.

If the process occurs in a crystal lattice, instead of an isolated center, expressions (23) and (24) corresponding to a single atom need to be slightly changed, following the above modification, by substituting the field of the crystal lattice for the atom field. The lattice Coulomb potential multiplied by the charge e_1 of the scattering particle is

$$U = \sum_i \frac{Ze_1 e}{|\mathbf{r} - \mathbf{r}_i|} \exp\left(-\frac{|\mathbf{r} - \mathbf{r}_i|}{R}\right) . \tag{25}$$

The summation is over all lattice atoms marked by the superscript i. For simplicity, exponential screening is used, with the screening radius

$$R = 0.885 Z^{-1/3} \frac{\hbar^2}{me^2} \,. \tag{25$'$}$$

The procedure reduces to multiplying the bremsstrahlung cross section for one atom by the interference factor:

$$\mathrm{d}\sigma = \mathrm{d}\sigma_{\mathrm{BG}} \left| \sum_i \exp \frac{\mathrm{i}\mathbf{q}\mathbf{r}_i}{\hbar} \right|^2 . \tag{26}$$

The enhancement effects related to the substitution of the crystal lattice potential for the Coulomb potential can best be represented if the Bethe–Heitler cross section σ_{BG} is given in terms of $\mathbf{k}$ (see formula (2.19) or Appendix 1 in Ref. [1]), where $\mathbf{q} = \hbar\mathbf{k}$ is the momentum transferred to the lattice in the process of bremsstrahlung and k_1 is the component of the vector $\mathbf{k}$ along the electron path.

In the case of a charged particle traveling at an angle θ to the crystallographic axis x of a rhomboid, tetragonal or cubic crystal, the probability of bremsstrahlung in the crystal can be computed if the integration over $\mathbf{k}$ in the expression for bremsstrahlung from a single atom (see formula (2.19) in Ref. [1]) is substituted by the summation with respect to discrete variables n, m, l. This is possible because a periodic medium admits only discrete momenta inversely proportional to the periods of the corresponding axes of the crystal lattice. This procedure reduces to the following substitution:

$$\int_\delta \frac{\mathrm{d}k_1}{k_1^2} \int \mathrm{d}k_2 \int \mathrm{d}k_3$$
$$\to \sum_{n,m,l} \frac{2\pi}{d} \left[\frac{2\pi}{d}\, n\cos\theta + \left(\frac{2\pi}{f}\, m \sin\alpha - \frac{2\pi}{b}\, l\cos\alpha \right) \sin\theta \right]^{-2} , \tag{26$'$}$$

where δ is the inverse of the coherence length (1), d, f, and b are the lattice constants, θ and α are the polar and azimuthal Euler angles, respectively, determining the positions of the coordinate axes k_1, k_2, k_3 associated with the particle motion relative to the crystal axes (Fig. 6). Using the Euler angles θ, α (for convenience, the third Euler angle η [1] is chosen to be zero) and the condition allowing the quantum momentum

$$k_x = \frac{2\pi}{d}\, n \,, \qquad k_y = \frac{2\pi}{f}\, m \,, \qquad k_z = \frac{2\pi}{b}\, l$$

to be transferred to the lattice along x, y, z axes, we obtain

$$k_1 = k_x \cos\theta + (k_y \sin\alpha - k_z \cos\alpha) \sin\theta \,.$$

Let us now consider the case where the coherence length is significantly larger than the crystal lattice constants. Then, the integral or the sum (26$'$) at $\delta \ll 1$ is determined by the region near the lower limit. The only difference is that, in the case of a crystal, integration must be replaced by summation over discrete variables of n, m, l. This leads to a substantial enhancement of bremsstrahlung in crystalline media compared with amorphous ones. Indeed, at certain parameter values, an additional factor $2\pi/d\delta \gg 1$ appears in the right-hand side of expression (26$'$), in contrast to its left-hand part, leading to a peaked pattern (main maxima) in the bremsstrahlung spectrum [1].

If an electron enters a crystal at a small angle to the x axis, i.e. at $\theta \ll 1$, the main maxima have $n = 0$ and m, l satisfying the condition

$$\left(\frac{2\pi}{f}\, m\sin\alpha - \frac{2\pi}{b}\, l\cos\alpha \right) \theta \geqslant \delta \,. \tag{27}$$

If it is possible to choose θ, m, l, α such that this condition be fulfilled, the bremsstrahlung enhancement in the crystal is maximum and occurs at incidence angles

$$\theta = \theta_{\mathrm{eff}} \approx \delta \left(\frac{2\pi}{f}\, m\sin\alpha - \frac{2\pi}{b}\, l\cos\alpha \right)^{-1} . \tag{28}$$

For a broad class of crystals, $\theta_{\mathrm{eff}} \sim 100\, mc^2/E$, which is significantly higher than the characteristic bremsstrahlung angles at $E \gg mc^2$. At $\theta = 0$, in which case the electron is incident parallel to the crystal axis, the main maxima in the CB spectrum are absent, and a sharp fall in the CB intensity occurs (the type-B case of CB dealt with below).

Among experimental works done after the publication of Ref. [1], studies by R Avakyan and his co-workers [92a] deserves special mention. They were fulfilled at the Physical Institute, Yerevan, and resulted in a record degree of CB polarization and monochromatism. In another series of studies conducted at a Japanese particle accelerator, CB was employed to determine, to within 2%, form factors for silicon and aluminium atoms [92b].

Interest in CB and in the creation of electron–positron pairs by photons with energies of 100–1000 MeV in diamond crystals reported in Ref. [93a] was stimulated by theoretical considerations [93b] which also became known after the monograph [1] was published. Reference [93b] dealt with the so-called type-B CB and pair formation (see Section 11.3 in [31] for more details). The results were used later to study radiation associated with channeling low-energy particles (see Section 8.2).

However, recent investigations into radiative processes demonstrated that the existing CB theory fails to explain many experimental findings. Channeling effects at low energies need to be taken into account (see Section 6.2) as well as effects due to the inapplicability of the Born approximation at ultrahigh energies (see Section 6.1). These

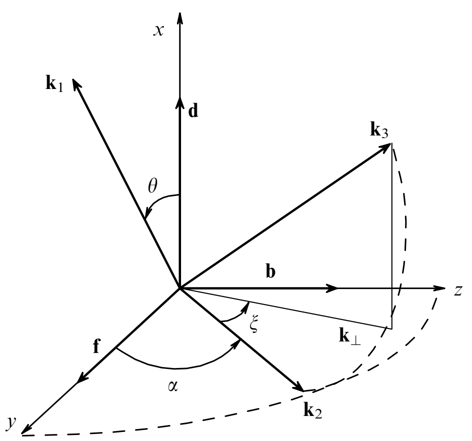

Figure 6. Relative positions of the axes of a rectangular lattice and the coordinate axes associated with the particle motion. The axes x, y, z are aligned with the lattice axes $\mathbf{d}$, $\mathbf{f}$, $\mathbf{b}$. The axis k_1 is parallel to the direction of motion. The angle θ is the entrance angle with respect to the axis x. The plane $\mathbf{k}_3, \mathbf{k}_2$ intersects the crystallographic lattice plane y, z along the line (of sites) $\mathbf{k}_\perp$. It is perpendicular to axes x and directed along vector $[\mathbf{x}\mathbf{k}_1]$. Angle α is the angle between axis y and $\mathbf{k}_2$; ξ is the angle between $k_\perp = (k_2^2 + k_3^2)^{1/2}$ and $\mathbf{k}_2$.

theoretical problems are considered at greater length in Sections 8 and 9 following the discussion of relevant experimental studies in Section 6.

At present, CB is extensively used in high-energy nuclear physics. It is therefore imperative to establish the limits of its applicability. Section 12 in Ref. [1] concerns CB in a thin crystal and considers the feasibility of using the Born approximation over a broader range. It is shown in Ref. [31] that the CB theory also holds beyond the Born approximation, up to very high energies of incident particles, at which the so-called constant-field radiation is emitted. Below, we will specially consider this limiting case, which has a deep-lying physical cause related to the introduction of the coherence length into the theory.

It is well known [9, 10] that charged particles passing through a crystal have their paths deflected by the lattice field, the more so the closer the particle approaches the crystallographic planes or crystal axes (see Sections 6 and 7 for details). Such motion, usually referred to as planar or axial channeling, respectively, is strongly dependent on the sign of the charge of the scattered particle (Figs 7 and 8). A positively charged positron is in periodic motion between the planes, whereas an electron, having a negative charge, intersects them. In the case of axial channeling, the electron coils about the axis, while the positron repulses from it. Channeling depends on the patterns of scattering on Coulomb centers, but the Born approximation used in Ref. [1] does not describe it. It is important that channeling can be characterized in terms of the classical field theory and corresponds to the classical particle behavior [9], while the scattering of particles in periodic structures, in which case interference processes acquire significance, reflects the wave properties of matter and requires a quantum treatment.

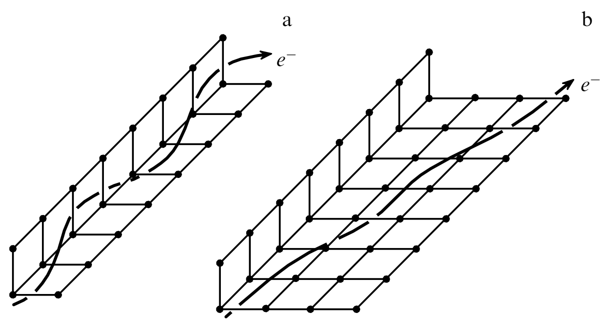

Figure 7. (a) Axial and (b) planar channeling of an electron [126].

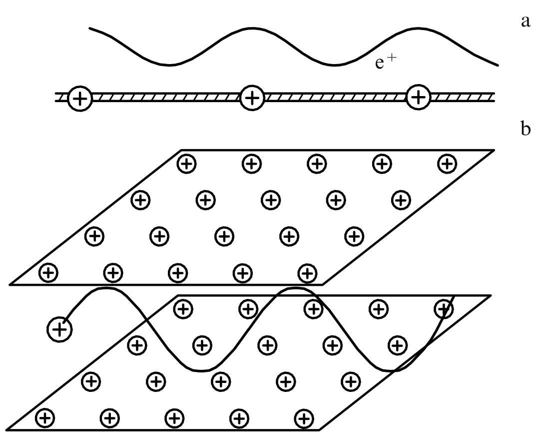

Figure 8. (a) Axial and (b) planar channeling of a positron.

Channeling processes are linked to motion in the crystal lattice field and have been a subject of low-energy nuclear physics [9, 10]. In the late 1970s, these studies were continued within the realm of high-energy radiation physics, mostly by Soviet scientists [8]. For simplicity, theoretical aspects of channeling as well as its effects on radiative processes are considered in Sections 7 – 9.

It is only natural that particles uninvolved in the channeling process radiate in an ordinary way. In other words, if the coherence length is smaller than the distances between Coulomb centers, the radiation corresponds to the Bethe – Heitler limit; in an opposite case, it takes the form of CB.

There is a criterion for the neglect of the channeling effect on radiation processes (see Sections 7 – 9 for details). In Fig. 9, θ denotes the angle between the electron momentum and axis x aligned with one of the crystal axes, φ is the angle between the momentum projection onto the plane y, z and axis y, and $\Phi = \theta \sin\varphi$ is the angle between the momentum $\mathbf{p}$ and plane y, z. It is worth noting that the angle φ is linked to the Euler angle α introduced above (see Fig. 6) by a certain relation.

The Lindhard angle is of importance in particle channeling within a wide range of energies, from nonrelativistic to ultrarelativistic ones. It was introduced into low-energy nuclear physics as

$$\theta_{\mathrm{L}} = \sqrt{\frac{2U_0}{\beta^2 E}}, \tag{29}$$

where E is the energy of the emitting particle and U_0 is the depth of the interplane, or axial, potential. If $\theta \ll \theta_{\mathrm{L}}$, either planar or axial channeling is realized, and the results of the CB theory must be revised. If the opposite inequality for angles $\theta \gg \theta_0$, where $\theta_0 = U_0/mc^2$, is fulfilled, the CB theory

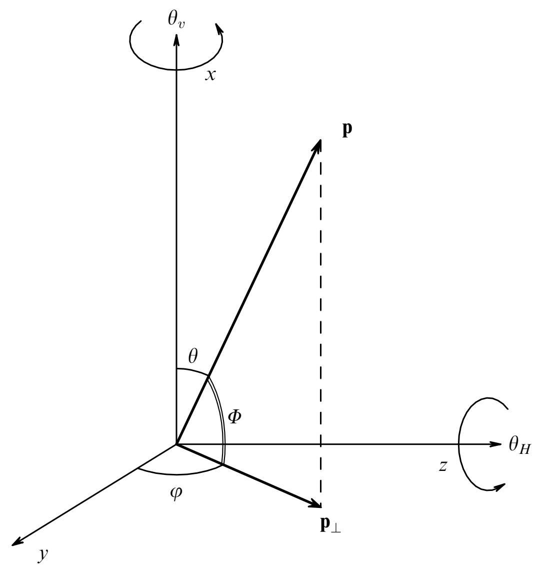

Figure 9. Relative orientation of the electron momentum and crystal axes. Axes x, y, z lie parallel to the crystallographic axes of the cubic crystal. The direction of motion of a particle having momentum $\mathbf{p}$ is determined by the polar angle θ to axis x; φ is the angle between the momentum projection onto the plane y, z and axis y. The tilt angle $\Phi = \theta \sin\varphi$ is the angle between $\mathbf{p}$ and plane y, z. The angle of rotation about the vertical axis x is $\theta_v = \theta\cos\varphi$; about the horizontal axis z, $\theta_H = \sin\varphi$.

remains valid. At $\theta \ll \theta_0$, on condition that $\theta \gg \theta_L$, magnetic bremsstrahlung takes place [30, 96, 17 – 19].

The first CB experiments showed that, if a particle entered a crystal at a small angle to the crystallographic plane, the radiation persisted although the CB theory predicted its disappearance (see formula (9.12) in Section 9 of Ref. [1]); type-B CB was not known at that time. This fact was introduced to me by N W K Panovskii of the Stanford University at the Kiev meeting in 1959 and by R Avakyan of the Physical Institute, Yerevan, at about the same time. Moreover, in the first work of Ref. [94] (1970), B Berman measured bremsstrahlung intensities produced by electrons and positrons with energies 16 – 28 MeV near the Lindhard angle, which proved to be different, at variance with the CB theory without particle-channeling effects taken into account. The authors ascribed this finding to channeling effects depending on the sign of the charge.

Since the mid-1970s, when the first theoretical works in this field were published [8], the situation has changed dramatically, which promoted further development of the bremsstrahlung theory taking into consideration channeling effects. In addition to the aforecited papers [94], R Avakyan and his co-workers published the results of their studies with positrons at energies of 2 – 16 GeV at the linear accelerator of the Stanford University and with 4.5-GeV electron beams at the cyclic accelerator in Yerevan [95a]. Figure 10 illustrates the considerable difference between the spectral distributions of CCB for positrons and electrons with an energy of 4.5 GeV in a diamond crystal.

Reference [95b] reports the orientation dependence of the electron and positron radiation at energies of 150 GeV in a germanium crystal for the case of axial channeling. The authors point out that the results are at variance with the CB theory only within a small angular region adjacent to the channeling axis. In this region, the radiation spectra begin to be dependent on the particle charge, and the electron radiation spectrum resembles the spectrum of magnetic bremsstrahlung in the quantum limit (see Section 9.3).

Radiation studies taking into account channeling processes are numerous. They are cited in reviews [12, 14 – 19], monographs [20 – 23, 27 – 31, 96], and the proceedings of recent scientific meetings [90, 91].

For the sake of simplicity, we will first review in brief the experimental data obtained in the latest studies and thereafter turn to their theoretical interpretation in Sections 7 – 9.

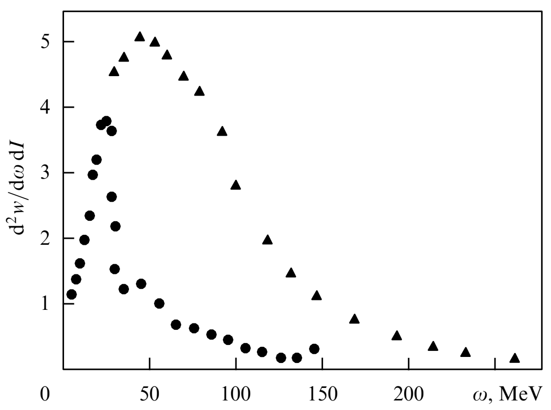

Figure 10. Spectral distributions of radiation by 4.5 GeV electrons (▲) and positrons (•) in planar channeling along the (110) plane of a diamond crystal [95a].

6. Radiation effects in channeling (experiment)

6.1 High energies

The probabilities of radiative processes in the crystal lattice field should differ considerably from those for CB if the emitting particle undergoes channeling (see below). In such a case, the radiation is sometimes also called CB [30]. However, it is convenient to denote it as CCB for the high-energy region, to emphasize that the effect of channeling is not to be neglected. Scientists of the USSR and former USSR have made the most important contribution to the development of the CCB theory [8, 12, 14 – 23, 27 – 31].

In order to understand the physical nature of this complex phenomenon, one should pass to the system of coordinates in which the emitting particle is at rest prior to collision and use the pseudophoton method to consider scattering of the crystal lattice field by a charged particle. To be specific, we will discuss the case of axial channeling. In accordance with Section 5, as $v \to c$, an emitting particle will be affected by the fields (compressed to a pancake shape) of linearly polarized plane waves of atoms arranged periodically on the crystal lattice axis (cf Fig. 5). Representing the electric field of the moving lattice as an integral over time and using the Compton cross section makes it possible to evaluate the probability of emission in the Born approximation, as shown in Section 5, and for axial channeling (see Section 9 for details). Evidently, the probability of CCB beyond the Born approximation depends on the character of particle movements in the lattice field, which is in turn determined by the parameters of the lattice, the particle velocity direction relative to the crystal lattice axes, and its charge. A similar line of reasoning appears to be valid for radiation in the case of planar channeling. However, the physical nature of this phenomenon is much more complicated than that of CB even though CCB turns to CB provided the conditions indicated at the end of Section 5 are fulfilled. Theoretical aspects of orientation effects will be discussed at greater length in Section 7, while Sections 8 and 9 concern theoretical studies of radiation channeling effects.

Unlike CB, the spectral distributions of electrons and positrons differ considerably owing to differences in the patterns of their motion in the crystal lattice field. In recent years, the results of high-energy experiments and theoretical studies have mainly been compared in the framework of the quasi-classical CCB theory developed by a group of theorists at the Institute of Nuclear Physics, Novosibirsk [30]. Data on the creation of electron – positron pairs have been compared in the context of the work of researchers from Minsk [18] and Ref. [97]. Unfortunately, these studies are mathematically too complicated to be reproduced in this review (see Section 9).

The basic physical results were independently obtained by Lindhard [98], who used a slightly modified pseudophoton method and interpreted the earlier experiments that had demonstrated for the first time pronounced bursts of hard photon emission attributable to magnetic bremsstrahlung [99]; for these bursts, the Bethe – Heitler cross section was exceeded by a factor of 50. True, another work of the same authors revealed the ambiguity of this effect due to multiple photon emission (see below).

In Ref. [100], the theory [30] was applied to the analysis of electron radiation spectra under the conditions of the transition from the axial to planar target orientation taking

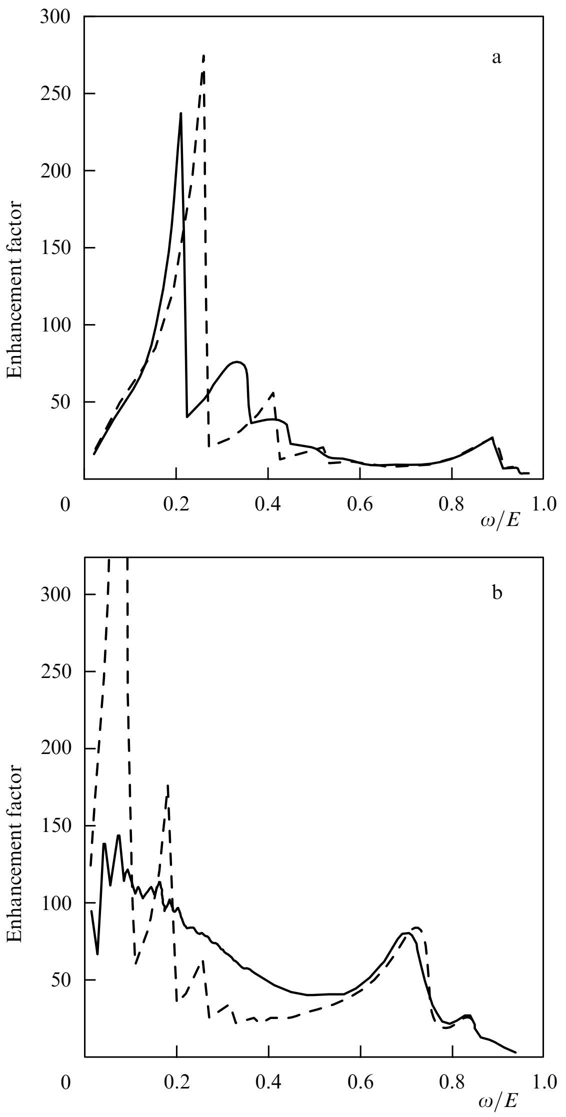

Figure 11. Enhancement factors of the CB (solid lines) and CCB (dashed lines) intensities generated by 200 GeV electrons entering a crystal at angles of (a) 0.0006 rad and (b) 0.0002 rad depending on ω/E. The angle φ to the (110) plane was 0.04 rad in both cases.

into account the mutual influence of neighboring atomic chains. Figures 11a, b show the CB and CCB enhancement factors plotted against the emitted photon energy at different energies and angles of electrons at which they enter a crystal when channeling effects are pronounced.

Reference [101] reports the degree of polarization computed in terms of the classical [30] and CB theories depending on the emitted photon energy at different angles of entrance. The calculations are made for the transition zone where the CB theory is already inapplicable but the constant-field approximation is not yet reached. The results are presented in Fig. 12a, b together with the corresponding plots for the probabilities of the processes. The plots are courtesy of S Darbinyan and N Ter-Saakyan of the Physical Institute, Yerevan. They indicate that the two theories (at the numerical parameters used for the calculation) yield virtually identical results for photons having energies comparable with the energy of the emitting particle. At $\hbar\omega/E < 0.4$, the enhancement coefficients and the degree of polarization are significantly different.

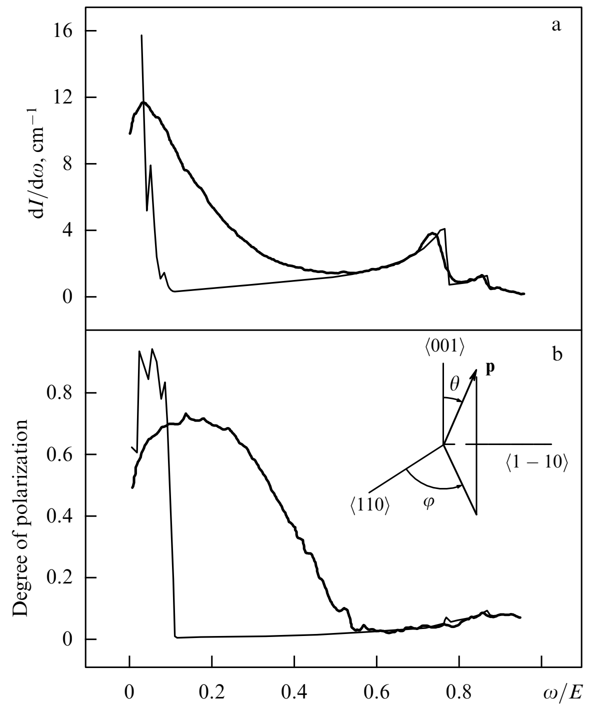

Figure 12. Theoretical curves of (a) spectral intensity and (b) the degree of polarization in the process of electron channeling, obtained using a semiclassical theory (thin lines) and the theory of coherent bremsstrahlung (thick lines) depending on ω/E. The electron energy was 150 GeV, the tilt angle $\varphi = 0.005$ rad, and the angle of incidence $\theta = 0.0003$ rad.

Experimental data obtained at CERN with emitting particles of 70, 150, and 240 GeV that entered diamond and silicon crystals at angles of 0.1 – 1.0 mrad to their axes confirmed, by and large, the results of the theory [30]. An emitting particle of 150 GeV energy experiences the action of a field of approximately 10^{16} V cm^{-1} in the frame of reference in which this particle is at rest. Since the transverse motion of the particle during emission is small, the particle remains virtually all the time in a constant magnetic field. In these conditions, the radiation should correspond to synchrotron radiation in very strong fields. This limiting case is known in the literature as the constant-field approximation [17, 30, 103]. A detailed analysis of this situation is presented in Section 9.

The experiment was conducted by a large group of scientists from different countries — Denmark, Switzerland, Italy, South Africa, and Armenia [102] — and demonstrated isolated peaks due to the emission of individual photons in a diamond crystal, 50 times in excess of the Bethe – Heitler radiation. The investigators examined the region of the transition from CB to CCB depending on the relationship between the angle of entrance of the particle into the diamond crystal and the Lindhard angle. They proposed to use the results of the experiment for the formation of quasi-monochromatic photon beams with energies of hundreds of gigaelectronvolts.

The joint study was continued to include the investigation of the coherent formation of electron – positron pairs under conditions of channeling in a single silicon crystal at photon energies of the order of 150 GeV [103]. The measured probability of pair production for photons with $40 < E < 130$ GeV was up to 6 times the Bethe – Heitler probability, in excellent agreement with the calculations based on the quasi-classical theory in the constant field approximation [30]. However, there was a marked discrepancy between the measured and calculated values at energies higher than 130 GeV. Therefore, additional arguments are needed to explain the experimental findings. (The work was presented at the Workshop in Tabarz.)

In this context, it is worth mentioning an earlier experiment [104] on the coherent pair formation in a germanium crystal at photon energies of 20 – 150 GeV for directions of the pair motion close to the $\langle 110 \rangle$ crystal axis. The experiment was prompted by the theoretical reasoning of Ref. [97a]. However, it used a thick crystal which might be contaminated by multiple CCB processes, although corrections were introduced. The measured and calculated [97b] probabilities of electron – positron pair formation are compared in Fig. 13.

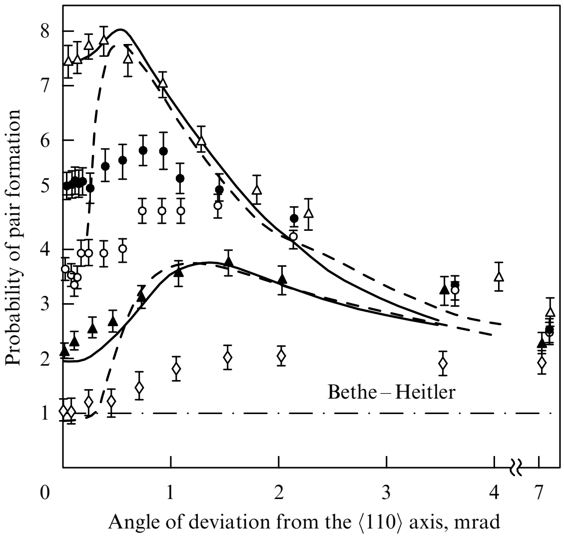

Figure 13. The probability of electron – positron pair formation in axial channeling in units of the Bethe – Heitler probability depending on the angle of deviation from the $\langle 110 \rangle$ axis. Photon energy range: △, 120 – 150 GeV; ●, 90 – 120 GeV; ○, 60 – 90 GeV; ▲, 40 – 60 GeV; ◇, 22 – 40 GeV. Dashed line: coherent theory of pair production; solid line: quasi-classical theory [104].

Experiments with polarized photons of bremsstrahlung at energies of a few hundred gigaelectronvolts are believed to be of primary importance for particle physics. Over the past 30 years, CB has been extensively employed to produce linearly polarized photon beams in experiments with elementary particles. In the past decade, the so-called 'spin crisis' problem required the production of circularly polarized beams. One of possible ways to obtain such beams is to transform their linear polarization into a circular one by means of coherent e^+e^- pair formation in a thick crystal. This approach, suggested by N C Kabibo, is underlain with the dependence of the pair-production cross section in a crystal on the direction of linear polarization with respect to the crystal plane. This means that the first thing to do is to obtain linearly polarized beams with energies of 100 – 150 GeV. Experiments at CERN using 200 GeV electrons showed that, with a suitably oriented diamond crystal, it is possible to produce linearly polarized photons with a peak energy of 150 GeV, in conformity with the CB theory. An experiment on the transformation of linearly to circularly polarized photons designed by the same group of physicists is currently underway at CERN (R Avakyan, private communication).

Another CERN collaboration has recently brought about interesting data on the generation and detection of photon polarization in the multigigaelectronvolt energy range during channeling [105].

It was known from previous studies [106] that in the case of planar channeling photons exhibit a 100% polarization in a CCB process at significantly lower electron energies. It proved equally true of situations with high electron energies [107].

In a study prompted by a group of investigators (see [109] and the references therein) and reported in Ref. [108], axial channeling radiation was employed to produce positrons in a tungsten crystal 1.2 mm in thickness (equivalent to a few radiation lengths). The use of CCB resulted in a 3 – 3.5 times higher enhancement of photon intensity in the given energy range compared with the magnetic bremsstrahlung in an amorphous medium.

The angular distribution of hard photons produced by 1.2 GeV electrons in a single crystal of silicon in the case of axial channeling was analysed in Ref. [110]. This work continued the previous studies of the same authors [111] in which they had investigated radiation intensity of channeled electrons in a range of energies from 200 to 1100 MeV at two angles of entrance into a silicon crystal, $\theta = 0$ and $\theta = 2°$.

Channeling processes and related events in the gigaelectronvolt range were reviewed in Ref. [96]. Reference [112a] predicted a CCB enhancement due to the decay of energy levels in the plane perpendicular to the particle motion. This prediction was confirmed in a later study of pair production in a germanium crystal [112b].

The results of theoretical research on electromagnetic processes in oriented single crystals at high energies and the cascade theory were presented at recent conferences [90, 91] and in monographs [30, 31]. Evidently, these processes are much more complicated than those discussed above. Time is needed to study them in theory and experiment.

6.2 Low energies

The theory of radiative processes at energies below several tens of megaelectronvolts taking into account channeling is substantially different from the theory of similar processes at high energies and defies a simple theoretical description (see Section 8). As early as, in 1965, Lindhard discovered the equations of motion for channeled particles at low energies [113], which are successfully used in low-energy physics. For the first time, the Lindhard theory found experimental confirmation in a work of Uggerhoj [114]. The results of studies in low-energy nuclear physics performed at that time have been summarized in numerous publications references to which can be found in Refs [9, 10a].

In a later period channeling became the subject-matter of experimental and theoretical studies devoted to electromagnetic interactions. Their results are reviewed in Ref. [10b]. The early publications that contributed to the theory of radiation by channeled particles [8] and the first experimental results in support of theoretical predictions [115] eventually opened a new avenue of research related to electromagnetic processes associated with channeling — CR.

It should be noted that the theory of channeling, originally developed for the analysis of problems pertaining to low-energy nuclear physics, is currently applied to solid-state spectroscopy [15]. It was minutely discussed in Refs [113, 116, 117] and is given much attention in the latest review [31], which also contains references to the relevant literature.

Experimental studies of CR at emitting-particle energies lower than a few tens of megaelectronvolts were initiated in Denmark (Arhus), USA (Stanford University), and Armenia (Physical Institute, Yerevan) [115]. They have been greatly intensified over the last years by the joint efforts of German physical centers (Darmstadt, Munich, etc.).

It has been mentioned above that there are two limiting cases of channeling, axial and planar channeling. In the former, a particle is captured into the channeling regime and travels parallel to the crystal axis undergoing the influence of the axisymmetric Coulomb field of the axis. In the latter case, a particle is under the action of the Coulomb fields of the atoms located on the plane (see Fig. 8). Evidently, the motion patterns depend on the charge of the particle. If the particle momentum changes slightly (that is, if the effective distances are, according to the Heisenberg uncertainty relation, large compared with the characteristic size of a unit cell in the crystal lattice), the channeled particle does not feel the discreteness of the field produced by the lattice axes or planes and travels in the field of the averaged potential (introduced by Lindhard).

A channeled particle in the averaged potential field exhibits discrete energy levels in the plane normal to the direction of motion. Radiative transitions between transverse-energy levels, which are in the atomic energy region, are responsible for the appearance of hard photons following the transformation to the laboratory system of coordinates (see Section 8 for details). This class of radiation, first predicted and investigated by M Kumakhov and other physicists, mainly in the USSR [8], is called radiation by channeled particles or simply channeling radiation (CR) [27, 28, 31, 115, 117] (see Section 8 for details).

Reference [118] compares CR and DXR characteristics in a diamond crystal in an energy range from 3 to 9 MeV. Under identical experimental conditions, the intensity of CR turned out to be three orders of magnitude greater than that of DXR notwithstanding almost complete absence of background radiation associated with DXR.

A recent publication [119a] describes the concomitant emission of CR and DXR in diamond and silicon crystals at an electron energy of 4 MeV. As in a preceding study [119b], this experiment revealed an interference pattern in DXR directions, which was confirmed by calculations [19a] based on the kinematic theory of DXR.

Planar channeling of electrons with energies ranging from 5.9 to 9.0 MeV in natural diamond single crystals of thicknesses 13, 20, 30, and 55 μm was studied in Ref. [120]. Since radiation reproduces the temporal structure of an electron beam, it is possible to obtain a source of γ radiation that operates for picoseconds. Moreover, radiation in planar channeling has a number of other important characteristics, such as high intensity (10^{12} photon s^{-1}), small spectral width, and good adjustability in the 10 – 40 keV range, which have various practical implications.

It was demonstrated [121] that the CR in the case of planar channeling should be linearly polarized. This inference found experimental confirmations [122, 123]. The authors of Ref. [123] observed discrete transition lines in the case of both planar and axial channeling of emitting electrons with an energy of 62 MeV (Fig. 14).

Reference [124] examined CR in planar and axial channeling of electrons with an energy of 6.9 MeV in a

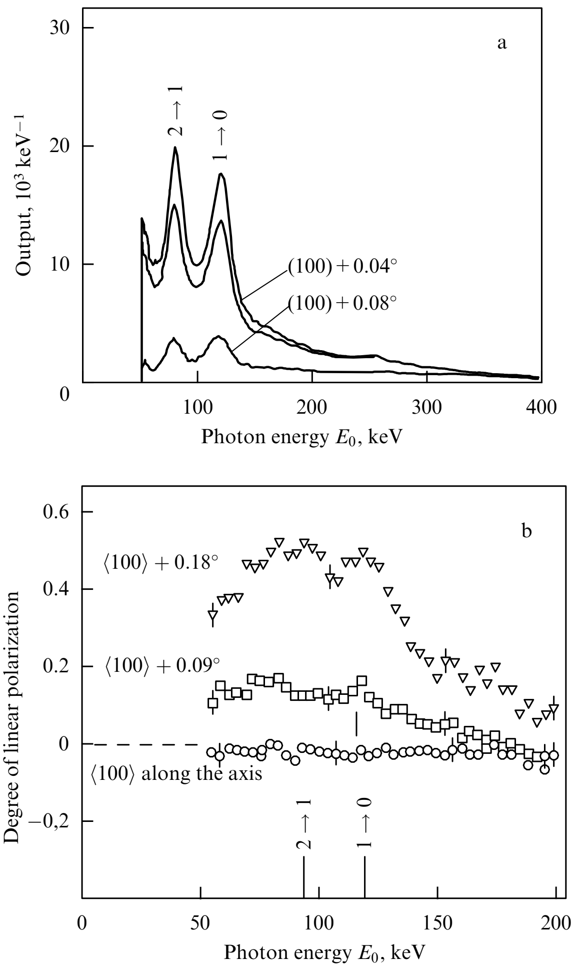

Figure 14. (a) Intensity of the radiation of channeled electrons in the (100) plane of a single silicon crystal depending on the energy of the emitted photon at various tilt angles φ. The electron energy is 62 MeV. The figure shows transitions between discrete energy states of the channeled electrons. (b) The degree of linear polarization during axial channeling along the ⟨100⟩ axis of a single silicon crystal at minor deviations from the axis depending on the emitted photon energy [122, 123].

germanium crystal and compared it with the calculated CR at low energies.

Linearly polarized CR in the megaelectronvolt energy range produced by electrons accelerated to an energy of 1 GeV was observed in Ref. [125]. As expected, no discrete lines associated with channeling radiation could be distinguished. Reference [126] analysed angular-spectral and polarization characteristics of CR and inspected more complicated situations in which a transition from purely axial to planar channeling occurred and the CB frequencies overlapped the radiation frequencies of channeled particles. For instance, it was shown [126] that the CR associated with channeling along the ⟨110⟩ axis exhibited partial linear polarization, but did not have such polarization if channeling occurred along the ⟨100⟩ axis which displayed rotational symmetry.

Reference [127] reports a study of the temperature dependence of radiation parameters in planar channeling of electrons with an energy of 62.8 MeV in single crystals of silicon, germanium, and beryllium in the 12 – 330 K range. The authors measured transition energies varying from 40 to 240 keV and line widths of transitions between the energy levels of the averaged potential field in the crystal. The experimental findings were used to determine the Debye temperatures.

A review of experimental and theoretical studies can be found in Refs [128, 15, 27, 28].

7. Orientation effects and channeling of charged particles in crystalline matter

7.1 Coulomb scattering cross sections

The motion of a relativistic particle in the crystal lattice field depends on Coulomb scattering by crystal atoms. The particle interacts coherently with the lattice atoms periodically arranged along the direction of its motion if the corresponding coherence length (see Section 7.2) is of the order of or larger than the lattice period. The resulting interference phenomena depend on the phase relations between different acts of electron wave scattering by periodically arranged atoms and the directions of their motion with respect to the crystal axes. In what follows, these phenomena will be referred to as orientational ones and will be given a quantum treatment. This qualitatively changes the pattern of scattering in periodic media compared with homogeneous amorphous materials in which interference does not occur. Expression (42) serves to illustrate this assertion. Indeed, when the amplitude of thermal fluctuations is larger than the coherence length of the corresponding processes (see Section 7.2), the interference processes decay exponentially and only the amorphous part of the cross section remains. In heterogeneous amorphous media, interference processes do occur due to fluctuations of various physical parameters (temperature, density, etc.) and cause photon emission by charged particles. This should, however, be the subject of a publication concerning radiative processes in amorphous materials.

In the present section, we will try to consider, in simple terms, orientation phenomena associated with scattering of charged particles in crystals, in the context of Ref. [129]. For simplicity, the Born approximation will be used throughout.

Let us summarize the elementary scattering cross sections that will be used below. The cross section of the Coulomb scattering on a single atom in the Born approximation, i.e. at $Ze^2/\hbar v < 1$, for charged relativistic particles with a spin of $1/2$ (the Mott formula) [130], supplemented by exponential screening, has the form

$$d\sigma_{\mathrm{M}} = \frac{4(Ze^2)^2E^2}{c^4(q^2+\hbar^2/R^2)^2}\left(1-\frac{q^2c^2}{4E^2}\right)dO' , \tag{30}$$

$$\mathbf{q}^2 = (\mathbf{p}-\mathbf{p}')^2 = \left(2p\sin\frac{\vartheta}{2}\right)^2 , \tag{31}$$

where $\mathbf{p}$, $\mathbf{p}'$ are the particle momenta before and after the scattering; ϑ, φ are the polar and azimuthal scattering angles; Z is the charge of the nucleus; R is the screening radius (25$'$); and $dO' = \sin\vartheta\, d\vartheta\, d\varphi$.

Evidently, the cross section (30) obtained in the first Born approximation is independent of the charge of the scattered particle. Conversely, the scattering cross section in the next Born approximation depends on the sign of the charge even though only minor corrections are needed. This is at variance with experimental data that suggest a strong dependence on the particle charge in CB processes [94, 95]. It has been mentioned in Section 6 that this discrepancy is due to channeling, first considered by Lindhard [9]. This problem will be dealt with at greater length below.

However, except channeling effects which depend on the charge of the particle and can be explained in terms of classical electrodynamics, experiments reveal interference processes responsible for orientation effects and requiring a quantum treatment. It should be noted that the use of the eikonal approximation can greatly promote the development of the theory of orientation phenomena and channeling in both limiting cases (see monographs [31, 21] and the literature cited there).

For simplicity, we will use the Born approximation which, due to unique properties of the Coulomb interaction, sometimes gives a correct answer even beyond the formally established limits of its applicability. For example, it was shown in Ref. [130] that the Mott formula (30) has a wider range of applicability than that determined by the Born condition. In the non-relativistic limit, formula (30) transforms into the known Rutherford formula, which has the same form in both classical nonrelativistic and quantum nonrelativistic mechanics in the case of accurate calculations (i.e. without the use of the Born approximation).

It follows from expressions (30), (31) that the overwhelming majority of scatterings over a wide energy range occur at small angles ϑ, of the order of $\hbar/pR \ll 1$ or smaller. It is therefore possible to neglect the last multiplier in (30) which takes into account the electron–atom spin interaction. Then, formula (30) for small scattering angles ($\vartheta \ll 1$) becomes identical with the known relativistic Rutherford formula of classical electrodynamics [131].

To sum up, the original formulas used below to describe Coulomb scattering at small angles remain valid over a broad range of scattered-particle energies, from nonrelativistic to ultrarelativistic. Of course, this conclusion holds for the Coulomb field with the electron-shell screening field neglected, although in this case it is sometimes also possible to argue, based on the eikonal approximation, for the use of the Born approximation over a broader range. In the forthcoming discussion, the corresponding scattering cross section will in some cases be marked by the subscript RM.

7.2 Coherence length

This section is centered on the discussion of the coherence length in Coulomb interactions. The space region in which atoms act coherently depends on the coherence length for Coulomb scattering processes introduced in 1953 [129].

It follows from formulas (30), (31) that the principal contribution to the scattering cross section comes from small angles. The momentum transferred to an atom in this situation is $|\mathbf{q}| = 2p\sin\vartheta/2 \approx p\vartheta$. The momentum transferred perpendicular to the direction of the particle motion is $q_\perp \equiv \Delta p_\perp = p\sin\vartheta \approx p\vartheta$; that transferred parallel to the motion is $q_\parallel = 2p\sin^2\vartheta/2 \approx p\vartheta^2/2$. Since, in accordance with the RM scattering cross section, most particles are scattered at characteristic angles of order $\hbar/pR$, the momenta transferred to the atom both normal and parallel to its motion will be of the order of

$$\Delta p_\perp \approx \frac{\hbar}{R} , \qquad \Delta p_\parallel \approx \frac{\hbar^2}{pR^2} . \tag{32}$$

In accordance with the Heisenberg uncertainty relation, the effective longitudinal and transverse distances corresponding to these momenta have the following order of magnitude:

$$L_{\rm coh} = L_{\parallel} \approx \frac{pR^2}{\hbar}\,, \qquad L_{\perp} \approx R\,. \tag{33}$$

It is important to emphasize that the effective distances along the particle motion increase with increasing particle momentum and can reach macroscopic values at high energies. Therefore, if this length (termed coherence length or formation zone for the Coulomb scattering process [129, 1]) harbors many atoms, they act together coherently and lead to orientation effects. This was first demonstrated in a study of scattering from a two-atom molecule I_2 in the Born approximation (justified in this particular case) [129, 1]. It turned out that the mean square of the angle of scattering by the molecule (corresponding to the scattering cross section) is four rather than two times that for scattering by an individual atom, if the molecule is oriented along the particle motion. This appears to have been the first prediction of orientation effects at high energies.

Evidently, this is true of the bulk of the particles scattered within characteristic scattering angles. In scattering at larger angles, the corresponding coherence lengths decrease; in the large-angle limit, both scattering and associated reactions should occur on individual atoms.

Of special interest for considering more complex processes is the introduction of the coherence length in the case of inelastic Coulomb scattering. Let us introduce, proceeding from the laws of conservation of energy and momentum, the coherence length for an arbitrary inelastic process characterized by a high directionality and consider, by way of example, reactions induced by Coulomb scattering. Let us further suppose that the scattering of a charged particle, with an initial speed $\mathbf{v}$, from an atom results not only in the transfer of a momentum $\mathbf{q}$ to the atom but also in the emission of a photon, which carries away an energy $\hbar\omega$ and a momentum $\hbar k = \omega\sqrt{\varepsilon}/c$, where ε is the dielectric permittivity of the medium to be maintained because of the longitudinal medium-density effect [132; 1, Section 14]. In addition, an arbitrary inelastic process may occur simultaneously, the energy Q_0 of which should be significantly smaller than the energy of the emitting particle. Using the laws of conservation of energy and momentum and neglecting the atom's recoil energy yield the coherence length

$$E - E' = \hbar\omega + Q_0\,, \tag{34}$$

$$\mathbf{p} - \mathbf{p}' = \hbar\mathbf{k} + \mathbf{q}\,, \tag{35}$$

where E, E', $\mathbf{p}$, $\mathbf{p}'$ are the particle's initial and final energies and momenta, respectively. We multiply the second equality by $\mathbf{v}$ and use the relation $\delta E = \mathbf{v}\delta\mathbf{p}$ to obtain, for minor energy changes,

$$vq_{\parallel} + \hbar kv\cos\theta' = \hbar\omega + Q_0\,. \tag{36}$$

For small emission angles of photons θ', the energy of which is much higher than atomic energies but smaller than the particle energy, we have

$$q_{\parallel} = \frac{\hbar\omega}{v}\left[1 - \frac{v}{c} + \frac{v}{c}\frac{\omega_0^2}{\omega^2} + \frac{v\vartheta}{2c}\left(\frac{\theta'}{2}\right)^2\right] + \frac{Q_0}{v}\,, \tag{37}$$

where ω_0 is the plasma frequency (10).

Expression (37) can be used to determine the coherence length of a given inelastic scattering process concomitant with processes of radiation and excitation and with the longitudinal density effect:

$$L_{\rm coh} = \frac{\hbar}{q_{\parallel}}\,. \tag{38}$$

The difference between this expression and (32) is responsible for various consequences in the consideration of physical phenomena. Specifically, if several competing processes of different coherence lengths occur concurrently on an atom, the ratio of their probabilities in the medium can differ significantly from that for one center.

7.3 Coherent scattering in a cubic crystal (orientation effects) and axial channeling

The elastic-scattering cross section (30) integrated over the solid angle, which will be used in the forthcoming consideration of Coulomb scattering in three-dimensional periodic media, can be conveniently represented in the following form which explicitly takes into account energy conservation:

$$\sigma_{\rm RM} = \int {\rm d}\sigma_{\rm RM}\,{\rm d}O' = \frac{4(Ze^2)^2E}{v^2}\int\frac{\delta(E_p - E_{p'})}{p'q^4}\,{\rm d}\mathbf{p}'\,. \tag{39}$$

In the right-hand side of (39), the integration is performed over the phase volume

$${\rm d}\mathbf{p}' = {\rm d}p'_x\,{\rm d}p'_y\,{\rm d}p'_z = p'^2\,{\rm d}p'\,{\rm d}O'\,. \tag{40}$$

For simplicity, we will regard all atoms in the cubic lattice as identical and assume exponential screening. Then, if relations (39), (40) are taken into account, the elastic Coulomb scattering cross section in the Born approximation assumes the form [129]

$$\begin{aligned}{\rm d}\sigma = 4\,\frac{(Ze^2)^2E}{v^2}&\int\frac{\delta(E_p - E_{p'})\,{\rm d}\mathbf{p}'}{p'\left[(\mathbf{p}-\mathbf{p}')^2 + (\hbar^2/R^2)^2\right]}\\ &\times\left|\sum_i \exp\left[\frac{{\rm i}(\mathbf{p}-\mathbf{p}')\mathbf{r}}{\hbar}\right]\right|^2,\end{aligned} \tag{41}$$

where the integral symbol refers to the integration over absolute values p'. It should be borne in mind that Ref. [129] was concerned with the ultrarelativistic case, which accounted for c^2 instead of v^2 in the denominator of the original formula (8) in that work and the omission of the symbol of integral over ${\rm d}p'$. Also, the mean square of the coherent (interference) scattering angle was introduced and minutely discussed in Ref. [129]. The resultant expressions can easily be applied to the study of Coulomb scattering cross sections, the subject of the following discussion.

Equation (41) differs from the conventional Mott cross section (30) containing a multiplier dependent on the spin of the scattered particle (which can be neglected at small scattering angles) by the presence of an interference factor, which should be averaged with the aid of the crystal's original wave function in order to take into account inelastic collisions [129, 1]. The result is well known and consists in the substitution of the interference factor by the following expression (such a substitution was validated in

Refs [129, 1]):

$$\left|\sum_i \exp\left[\frac{\mathrm{i}(\mathbf{p}-\mathbf{p}')\mathbf{r}_i}{\hbar}\right]\right|^2 = N\big[1-\exp(-2M)\big] + \exp(-2M)\left|\sum_i \exp\left[\frac{\mathrm{i}(\mathbf{p}-\mathbf{p}')\mathbf{r}_{i0}}{\hbar}\right]\right|^2, \tag{42}$$

where $\mathbf{r}_{i0}$ stand for the equilibrium positions of lattice atoms, N is the total number of atoms in the crystal,

$$2M = \frac{|\mathbf{p}-\mathbf{p}'|^2\,\overline{u^2}}{\hbar} \tag{43}$$

is the Debye–Waller thermal factor, and $\overline{u^2}$ is the mean square of the amplitude of thermal fluctuations of crystal atoms.

It follows from these expressions that the total scattering cross section breaks down into two parts: $\sigma = \sigma_{\mathrm{am}} + \sigma_{\mathrm{coh}}$. The first term corresponds to the ordinary Rutherford–Mott scattering cross section in an amorphous medium multiplied by $1-\exp(-2M)$:

$$\mathrm{d}\sigma_{\mathrm{am}} = N\big[1-\exp(-2M)\big]\,\mathrm{d}\sigma_{\mathrm{RM}}\,. \tag{44}$$

The second term describes the interference (coherent) scattering cross section, which will further be considered for a cubic crystal:

$$\mathrm{d}\sigma_{\mathrm{coh}} = \mathrm{d}\sigma_{\mathrm{RM}}\left|\sum_i \exp\left[\frac{\mathrm{i}(\mathbf{p}-\mathbf{p}')\mathbf{r}_{i0}}{\hbar}\right]\right|^2 \exp(-2M)\,. \tag{45}$$

The amorphous cross section contributes to all electron scattering processes in matter. The contribution is proportional to the number of atoms. In other words, any process associated with coherent scattering is accompanied by an analogous incoherent process. The present section is not specially concerned with the contribution of the amorphous cross section. We only point out that, in the adopted approximation, the summation of amorphous and interference scatterings leads to an ordinary expression for the scattering cross section in amorphous media if the interference scattering cross section is averaged over all possible directions from which particles enter the crystal.

Such a division suggested in Ref. [129] is now accepted by many authors. However, expression (42) may need revision for the purpose of considering more intricate phenomena, such as radiative process associated with the transition of atoms or even nuclei to excited states, the effect of additional external factors on the location of atoms in a crystal lattice, etc. The revision will require more precise experiments in the high energy range, especially when the predominant Coulomb interaction occurs in conjunction with other interactions.

The total coherent (interference) scattering cross section after the introduction of the above transformations and integration of (45) over the phase volume (using, in accordance with (40), new variables instead of angular ones for the convenience of further analysis) can be presented in the following form:

$$\sigma_{\mathrm{coh}} = \int \mathrm{d}\sigma_{\mathrm{RM}}\left|\sum_i \exp\left[\frac{\mathrm{i}(\mathbf{p}-\mathbf{p}')\mathbf{r}_{i0}}{\hbar}\right]\right|^2 \exp(-2M)\,p'^2\,\mathrm{d}p'\,. \tag{46}$$

Upon the integration over p', Eqn (46) without interference and thermal factors coincides with expression (30) devoid of the correction coefficient related to the particle spin. This allows it to be used over a broader range, i.e. outside the Born approximation limits.

For the elementary inspection of coherence effects, we assume that a particle enters a cubic crystal with a lattice constant a at a small angle θ to the axis x. For simplicity, we neglect the structure factor; otherwise, it will lead to the appearance of a certain multiplier (see [1, p. 410]). Suppose that the crystal has the form of a film of infinite size in the plane y, z with N_1 atoms arranged along the axis x. In this case, at $\mathbf{p} \sim p_x$, i.e. if $\cos\theta \sim 1$, we have

$$\left|\sum_i \exp\left[\frac{\mathrm{i}(\mathbf{p}-\mathbf{p}')\mathbf{r}_{i0}}{\hbar}\right]\right|^2 = \lim_{\substack{N_2\to\infty\\ N_3\to\infty}} N_2N_3\left(\frac{2\pi}{a}\right)^2 \times \delta\left(\frac{p_y'-p_y}{\hbar} - \frac{2\pi}{a}\,m\right)\delta\left(\frac{p_z'-p_z}{\hbar} - \frac{2\pi}{a}\,l\right) \times \sin^2 N_1\left(\frac{p_x'-p_x}{2\hbar}\,a\right)\left[\sin^2\left(\frac{p_x'-p_x}{2\hbar}\,a\right)\right]^{-1}. \tag{47}$$

By means of substituting (47) into (46), integrating over p_x', p_y', p_z', and dividing by the film area S, we find the probability of scattering of ultrarelativistic particles

$$\frac{\sigma_{\mathrm{coh}}}{S} = 4\,\frac{(Ze^2)^2}{v^2pp_x'}\,n_2n_3\left(\frac{2\pi}{a}\right)^2 \times \sum_{ml}\frac{(2\pi/a)^2(m^2+l^2)+(p_x'-p_x)^2/\hbar^2}{\left\{(2\pi/a)^2(m^2+l^2)+(p_x'-p_x)^2/\hbar^2+1/R^2\right\}^2} \times \exp\left\{-\left[\left(\frac{2\pi}{a}\right)^2(m^2+l^2)+\frac{(p_x'-p_x)^2}{\hbar^2}\right]\overline{u^2}\right\} \times \sin^2 N_1a\,\frac{p_x'-p_x}{2\hbar}\left[\sin^2 a\,\frac{p_x'-p_x}{2\hbar}\right]^{-1}. \tag{48}$$

Here, n_2n_3 is the particle number density in the plane y, z, and p_x' is determined by the conditions

$$p'^2 = p^2\,; \qquad p_y' = p_y + \frac{2\pi\hbar}{a}\,m\,; \qquad p_z' = p_z + \frac{2\pi\hbar}{a}\,l\,, \tag{49}$$

i.e.

$$p_x'^2 = p_x^2 - \frac{4\pi\hbar}{a}(mp_y + lp_z) - \left(\frac{2\pi\hbar}{a}\right)^2(m^2+l^2)\,. \tag{50}$$

The values of m and l are restricted by the amplitude of thermal fluctuations, that is by the condition

$$\frac{2\pi\hbar}{a}\sqrt{m^2+l^2} \leqslant \frac{\hbar}{\sqrt{\overline{u^2}}}\,. \tag{51}$$

For the majority of crystals, the upper limit for m and l can be taken to be of the order of tens. Therefore, in the relativistic region $p_x' \approx p_x$. Function σ_{coh} has well-defined maxima, which appear if the condition

$$p_x' = p_x + \frac{2\pi\hbar}{a}\,n \pm \frac{2\hbar}{N_1a}\,, \tag{52}$$

where $n = 0, 1, \ldots,$ is fulfilled.

Combining (50) with (52) leads us to the condition for the appearance of maxima in the form

$$n\alpha + m\beta + l\gamma = \frac{2\pi\hbar}{pa}(m^2 + l^2 + n^2) \pm \frac{\alpha}{\pi N_1}\,, \tag{53}$$

where α, β, and γ are the direction cosines of the traveling particle with respect to the coordinate axes of the crystal lattice. If. for a given direction of entrance, there are such triples of integers n_i, m_i, l_i that condition (53) is satisfied, then

$$\frac{\sigma_{\text{coh}}}{S} = 4\left(\frac{Ze^2}{vp}\right)^2 n_2 n_3 N_1^2 \times \sum_{m_i l_i n_i} \frac{(m_i^2 + l_i^2 + n_i^2)\exp\left[-(m_i^2 + l_i^2 + n_i^2)/b^2\right]}{\left[m_i^2 + l_i^2 + n_i^2 + (a^2/4\pi^2 R^2)\right]^2}\,, \tag{54}$$

where

$$b^2 = \frac{a^2}{4\pi^2\,\overline{u^2}}\,. \tag{55}$$

If, on the contrary, condition (53) cannot be fulfilled, σ_{coh} becomes small (the factor N_1^2 being absent), and the main contribution to the Coulomb scattering in these directions comes from the amorphous scattering cross section (44).

In bremsstrahlung, this is manifest as strong bursts (peaks) in a certain frequency range for a given photon emission angle θ' [in accord with (27)], against the background of the amorphous bremsstrahlung component corresponding to the amorphous scattering cross section (44). These peaks are due to orientation effects, as illustrated by Figs 11 and 12 and also by experiment [1]. They are especially noticeable in the emission of soft photons, in which case the bremsstrahlung cross section can be represented as the product of the scattering cross section and the probability of bremsstrahlung. This is also confirmed by Figs 11 and 12.

A detailed analysis of intense-scattering directions is needed to ensure the straightforward application of formula (54). Specifically, their number, width, and location in the crystal lattice must be specified. Such an analysis [129] indicates that these directions are concentrated along the planes of the crystal lattice containing large numbers of atoms. Moreover, there is considerable overlap between individual maxima.

According to (54), the coherent scattering cross section is proportional to N_1^2. This explains why the scattered electron is deflected from the directions where condition (53) is fulfilled, and enters the region of directions where the scattering is small. This process may repeat, which makes it necessary to consider multiple scattering phenomena. We therefore confine ourselves to those directions for which condition (53) is fulfilled (directions of maxima). If a particle travels along axis x (i.e. $\alpha \approx 1$), condition (53) is satisfied for $n = 0$, and the probability of scattering (54) is should be summed over all admissible values of m and l limited by (51):

$$m^2 + l^2 \leqslant \frac{a^2}{4\pi^2\,\overline{u^2}} \approx 100\,.$$

The sum that appears in (54) can be represented in the form

$$A = \frac{4\pi^2 R^2}{a^2} \sum_{m,\,l=0}^{\infty} \frac{4\pi^2 R^2}{a^2}(m^2 + l^2)\left[(m^2 + l^2)\frac{4\pi^2 R^2}{a^2} + 1\right]^{-2} \times \exp\left(-\frac{m^2 + l^2}{b^2}\right) = \frac{4\pi^2 R^2}{a^2}\,C\,, \tag{54$'$}$$

where C is a quantity of the order of ten, weakly dependent on $\overline{u^2}$. The quantity $4\pi^2 R^2/a^2$ is 0.063 for tungsten and and 0.024 for lead. The quantity $(\overline{u^2})^{1/2}/a$ is 0.022 for tungsten and 0.042 for lead at zero temperature and 0.046 and 0.085, respectively, at the Debye temperature. At these values, the quantity C for tungsten is 28.76 at zero temperature and 14.33 at the Debye temperature. For lead, $C = 38.61$ and 14.21, respectively. In most crystals, the ratio of the lattice period to the screening radius R ranges from 10 to 40, whereas the ratio of the screening radius to the amplitude of thermal fluctuations does not exceed 10. These numerical estimates neglect the structure factor which must be taken into account for calculations in particular experiments. Normally, the crystals used in experiments have a diamond-like lattice for which the necessary characteristics can be found in Ref. [1].

The Born approximation used here is *a priori* violated if the Coulomb scattering cross section on a film (whose length along the particle motion is $N_1 a$) exceeds the sum of geometric cross sections of the atoms lying in the plane perpendicular to the motion of the particle. This leads to the shadowing effect [31] and to the impossibility of representing the particle wave function in the form of a plane wave of constant amplitude. Taking this fact into account requires going beyond the limits of the Born approximation and restricts the film size along the direction of the particle motion. From the condition

$$\sigma_{\text{coh}} = \frac{4(Ze^2)^2}{v^2 p^2}\,N_2 N_3 N_1^2 A < N_2 N_3 \pi R^2 \tag{56}$$

we find the admissible crystal size in the direction of motion:

$$N_1^2 < \frac{1}{16\pi C \theta_{\text{L}}^4}\,. \tag{56$'$}$$

Surprisingly, condition (56$'$) does not include the Planck constant. It should be fulfilled over a wide range of energies, from nonrelativistic to ultrarelativistic, and depends solely on the Lindhard angle (29).

The right-hand side of inequality (56$'$) must be much larger than unity in order that N_1 could become large. This imposes a restriction on the Lindhard angle, which must be sufficiently small. In other words, orientation effects can be manifest only if the Lindhard angle is smaller than unity, that is if channeling takes place. We will use the inequality (56$'$) to examine a one-dimensional crystal (string).

To this end, a three-dimensional crystal ought to be replaced by a one-dimensional chain of atoms periodically arranged along the x axis at a constant lattice period a (Fig. 15a). This approximation is frequently used in such problems and is called the one-dimensional-chain approximation, or string approximation [9]. We assume that the particle moves parallel to the x axis at a distance $\rho = (y^2 + z^2)^{1/2}$ from the string.

Coulomb scattering from a chain of atoms arranged along the x axis, i.e. in a one-dimensional crystal, was considered by Lindhard in his well-known review article [9]. Lindhard's study was undertaken in the framework of classical electrodynamics, i.e. at $Ze^2/\hbar v > 1$, with the evaluation of quantum effects. In essence, his approach was based on the division of interaction processes into processes directed parallel to the motion of a particle and those in a transversal direction, under the influence of the averaged potential introduced by Lindhard. All later studies in this field developed, to varying degrees, Lindhard's basic ideas set forth in Ref. [9].

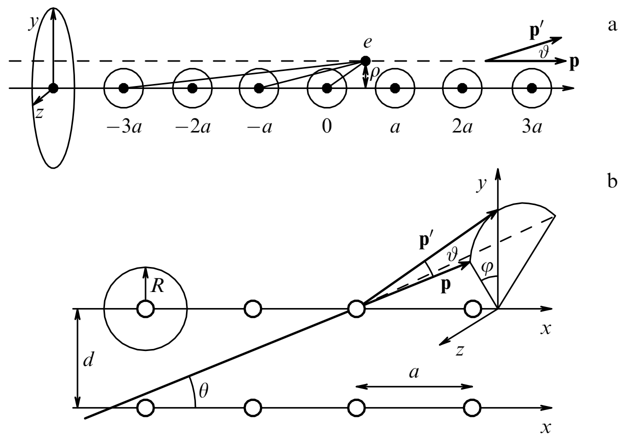

Figure 15. (a) Positron scattering in a one-dimensional crystal (string): a, distance between the neighboring scattering centers; ϑ, angle of scattering on the coherence length; ρ, distance between the particle trajectory and the string; $\mathbf{p}$ and $\mathbf{p}'$, the initial and final positron momenta. (b) Scattering of a charged particle intersecting the upper string at an angle θ. Angles ϑ and φ determine the direction of motion of the scattered particle with respect to the initial direction of momentum $\mathbf{p}$. R, d, a are the screening radius, distance between the neighboring strings, and string period, respectively (arbitrary scale). In this case, scattering actually occurs on several neighboring atoms because the particle traveling at an angle θ to the string axis enters the region of action (i.e. the sphere with a radius of the order of the screening radius) of only a few atoms.

If the number of atoms acting coherently in the scattering process is denoted by N_1, the applicability condition for the Born approximation assumes the form

$$\frac{N_1 Ze^2}{\hbar v} < 1\,. \tag{57}$$

In an opposite case, the classical approximation used by Lindhard is applicable.

The eikonal approximation can successfully be employed to study scattering from a chain of atoms at small angles, as shown in a number of publications (see [21] and especially [31] and references therein). In limiting cases, the eikonal approximation passes into the Born or the classical approximation and does not require that condition (57) or its opposite be fulfilled. The probability of scattering from a chain of atoms is easy to obtain from the above expressions. However, channeling-related processes require a different approach because they are strongly dependent on the charge of the scattered particle. We will employ the universally accepted approach [9].

The potential of a one-dimensional lattice (string) in the case of scattering of a positively charged particle by an atom is taken in the form (25). The probability of Coulomb scattering in the Born approximation is defined by the equation

$$\mathrm{d}\sigma = \frac{4(Ze^2)^2 E^2}{(q^2 + \hbar^2/R^2)^2}\left|\sum_i \exp\left[\frac{\mathrm{i}(\mathbf{p}-\mathbf{p}')\mathbf{r}_i}{\hbar}\right]\right|^2 \mathrm{d}O'\,, \tag{58}$$

where $\mathbf{r}_i = \rho - n_i\mathbf{a}$ is the distance of the moving particle from an atom with the coordinate $n_i\mathbf{a}$.

The interference factor for a one-dimensional chain is determined from the general expression (42) in which three-dimensional summation should be replaced by one-dimensional summation over atom numbers n_i; N_1 that appears in (47) is understood as the total number of string atoms in coherent interaction with the particle. It has been stated above that the number of atoms coherently participating in the scattering process is equal to the number of lattice atoms at the coherence length (33). For this reason, a string of total length $L > L_{\mathrm{coh}}$ should be divided into sections of length L_{coh} which should be regarded as one scattering center. A more detailed description of the scattering processes would be in conflict with the uncertainty ratio. This means that the classical consideration [9] is also applicable within certain limits linked to the uncertainty ratio.

Moreover, atoms of a one-dimensional lattice can be excited in the scattering process or undergo thermal fluctuations. Taking this into account leads, by analogy with what was considered in the preceding section, to the division of the interference factor into two parts, a coherent and an amorphous one.

The coherent interference multiplier for the problem under consideration, i.e. for motion parallel to the direction of the string, has the form

$$\left|\sum_i \exp\left[\frac{\mathrm{i}(\mathbf{p}-\mathbf{p}')\mathbf{r}_{i0}}{\hbar}\right]\right|^2 = \left|\sum_{i=0}^{N_1} \exp\left[\frac{\mathrm{i}q_{\parallel} n_i a}{\hbar}\right]\right|^2 = \frac{\sin^2 N_1 q_{\parallel} a/\hbar}{\sin^2 q_{\parallel} a/\hbar}\,, \tag{59}$$

where $\mathbf{r}_{i0}$ denote the equilibrium coordinates of atoms. Since $q_{\parallel} = p\vartheta^2/2$, scattering at $q_{\parallel} = \pi\hbar l/a$ (where l is an arbitrary integer) is observed at angles $\vartheta^2 = 2\pi\hbar l/pa$, and the interference multiplier turns into N_1^2. This effect corresponds to the rainbow scattering (see Ref. [31] for details). In this case, the shadowing effect can be avoided by means of satisfying the condition

$$\sigma_{\mathrm{coh}} \approx 4\left(\frac{Ze^2}{vp}\right)^2 N_1^2 A < \pi R^2\,, \tag{60}$$

which imposes a restriction on the length (i.e. the number of coherently acting atoms) of the one-dimensional chain:

$$N_1 < \theta_{\mathrm{L}}^{-2}\,, \tag{61}$$

where θ_{L} equals the Lindhard angle (29) to within a coefficient of the order of unity. This means that orientation effects are apparent (i.e. N_1 is larger than unity) only if the Lindhard angle is much smaller than unity. Otherwise, the lattice atoms act independently, and the theory of scattering remains valid without taking them into consideration. Thus, interference processes (leading to orientation effects) are closely related to channeling effects, as noted above.

8. Theoretical problems of low-energy radiative electromagnetic processes

8.1 Axial and planar channeling

Let us now consider the case of crucial importance where a moving charged particle crosses a chain of atoms. This case is important because such a particle, even in motion at a small angle to the chain, experiences the effect of an additional force acting in a transverse direction. Let us introduce the angle θ between the directions of the initial momentum $\mathbf{p}$ and the axis of the one-dimensional crystal harboring atoms with coordinates $\mathbf{r}_i = n_i\,\mathbf{a}$, where $\mathbf{a}$ is the string period. The angle between the planes containing $\mathbf{pp}'$ and $\mathbf{pa}$ is denoted by φ (Fig. 15b). Using the relation

$$(\mathbf{p}-\mathbf{p}')\mathbf{r}_i = pr_i\cos\theta(1-\cos\vartheta) - pr_i\sin\vartheta\sin\theta\cos\varphi$$

$$= pr_i\,\frac{\vartheta^2}{2} - pr_i\theta\vartheta\cos\varphi \qquad (62)$$

for small entrance and scattering angles, it is easy to note that the first and second terms in the right-hand part of (62) correspond to particle-momentum changes parallel and perpendicular to the velocity direction, respectively. Expression (62) enters into the interference multiplier (59) considered in the preceding section if only the first term in (62) is taken into account. Evidently, taking into account the second term in (62) leads to new important physical effects, first considered by Lindhard [9]. It has been stated above that the fundamental principles of channeling of charged nuclear particles were developed by Lindhard and his co-workers in the 1960s based on classical electrodynamics. In essence, Lindhard's approach relied on the division of interaction processes into processes directed parallel to the motion of a particle and processes that occur in a transverse direction under the influence of the averaged potential introduced by Lindhard. All later studies in this field developed, to a varying degree, Lindhard's basic ideas set forth in Ref. [9].

A particle moving at a small angle to a string experiences the action of the string's Coulomb field. This effect is due to the coherent action of atoms located within one coherence length. The coherence length can be determined for a specific process from the laws of conservation of energy and momentum. The results for Coulomb scattering are presented in Section 7.2. Following Lindhard, we introduce the averaged string potential acting in a plane transverse to the string,

$$U(y,z) = \frac{1}{L_{\mathrm{coh}}}\int\sum_i U_i(\rho-\rho_i)\,\mathrm{d}x\,, \qquad (63)$$

where $U_i(\rho-\rho_i)$ is the Coulomb potential of the ith atom multiplied by the charge of the scattered particle (25). Unlike the conventional Lindhard procedure, the averaging is performed over the string length comparable with the coherence length for a given process (in the present case, for the Coulomb scattering of electrons and positrons). In the case of large scattering angles (when the coherence length is smaller than the chain period), individual lattice atoms act independently of one another.

Equations of motion for a charged particle (quantum and recoil effects being neglected for the moment) have the form of normal classical equations in which the role of mass is played by relativistic mass [9, 31]:

$$\frac{\mathrm{d}}{\mathrm{d}t}\,\frac{m\mathbf{v}(t)}{\sqrt{1-\beta^2}} = -\nabla U(y,z)\,. \qquad (64)$$

In the transverse direction, they take the following form:

$$\ddot{\boldsymbol{\rho}} = -\frac{c^2}{E_\parallel}\,\frac{\partial}{\partial\boldsymbol{\rho}}\,U(y,z)\,. \qquad (65)$$

Here, the particle energies parallel ($E_\parallel$) and perpendicular ($E_\perp$) to the direction of motion are equal to

$$E \approx E_\parallel = c\sqrt{p_\parallel^2 + m^2c^2}\,, \qquad (66)$$

$$E_\perp = \frac{E\dot{\boldsymbol{\rho}}^2}{2c^2} + U(y,z) \qquad (67)$$

and can be regarded as independently conserved quantities. The transverse energy at $\rho > R$ can be represented as

$$E_\perp = \frac{E_\parallel\dot{\boldsymbol{\rho}}^2}{2c^2} = \frac{p_\perp^2c^2}{2E} = \frac{1}{2}\,E\theta^2\,, \qquad (68)$$

where θ is the angle between the velocity direction of the particle and the string direction.

Suppose that string atoms undergo small Gaussian deviations from the equilibrium

$$\mathbf{r}_n = \mathbf{r}_{n0} + \mathbf{u}_n\,. \qquad (69)$$

In this case, the averaged transverse potential

$$U(\rho-\rho_n) = \frac{1}{2\rho\overline{u^2}a}\int\mathrm{d}^2\mathbf{u}\exp\left(-\frac{\mathbf{u}^2}{2\overline{u^2}}\right)$$

$$\times\int\mathrm{d}x\,U(\rho-\rho_n+\mathbf{u},x)\,, \qquad (70)$$

where $\overline{u^2}$ is the mean square of the departures of atoms from their equilibrium positions in the string. If other forces act on the string atoms causing motion of their centers of gravity, the transverse potential should be averaged with the aid of the corresponding distribution function. Upon the integration, we have, for $\rho^2 \gg \overline{u^2}$,

$$U_0(y,z) = \frac{2Zee_1}{a}\,K_0\left(\frac{\rho}{R}\right). \qquad (71)$$

Here, R is the screening radius (25′) and K_0 is the modified Bessel function: $K_0 \approx 1$ at $\rho \sim R$ and rapidly decreases for $\rho > R$. It follows from the above expression that the behavior of a charged particle in a plane normal to the string depends on the averaged string potential which is of the order of atomic potentials. Expression (71) depends on the sign of the charge of the scattered particle e_2. In the case of an electron, the potential is negative. This accounts for the qualitative difference in the behavior of particles with opposite signs of charge, as repeatedly noted above (Fig. 16). Evidently, the Born approximation used in Sections 5 and 7 is inapplicable to the description of this class of phenomena.

A charged particle subjected to the averaged axial potential (63) may have discrete transverse-energy values. They can be found if an analogous problem is given a quantum treatment. In the case of axial channeling in the transverse plane, the Schrödinger equation has the form

$$\left[-\frac{\hbar^2}{2\gamma m_0}\left(\frac{\partial^2}{\partial^2 y}+\frac{\partial^2}{\partial^2 z}\right)+U(y,z)\right]\psi(y,z) = E_\perp\psi(y,z)\,. \quad (72)$$

Let us expand the potential energy into a series of vectors $\mathbf{g}_m$ which play the role of vectors of the reciprocal crystal lattice. The crystal is a set of periodically arranged parallel strings. Its averaged axial potential is a periodic function of

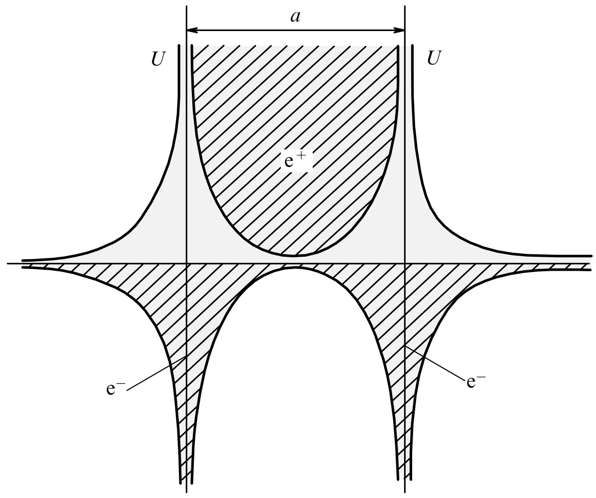

Figure 16. Potential energy (potential U) in a plane perpendicular to the direction of motion for a positron (top) and electron (bottom).

the variables y, z and can be represented in the form

$$U(\mathbf{r}_\perp) = \sum_{\mathbf{g}_m} U_{\mathbf{g}_m} \exp(\mathrm{i}\mathbf{g}_m \mathbf{r}_\perp) . \tag{73}$$

A solution to Eqn (72) has the form of Bloch functions with a normalization constant A_n and the wave vector $\mathbf{k}_\perp$ of the particle in a transverse plane:

$$\psi_n(\mathbf{r}_\perp) = \frac{1}{\sqrt{A_n}} \exp(\mathrm{i}\mathbf{k}_\perp \mathbf{r}_\perp) \sum_{g_m} C_m^n \exp(\mathrm{i}\mathbf{g}_m \mathbf{r}_\perp) . \tag{74}$$

The eigenfunctions and corresponding energy eigenvalues can be found using a standard procedure. By substituting (74) into Eqn (72), we obtain an infinite system of coupled equations for calculating the coefficients C_m^n. We restrict ourselves to a finite number of terms and reduce the problem to the solution of a system of N linear algebraic equations which is usually examined to find discrete energy levels in a transverse plane. In reality, discrete energy levels are Brillouin zones, due to the crystal periodicity, and the problem of their determination turns to a typical solid-state problem. Particularly, it was considered in detail in Ref. [124] for the case of electron axial channeling in a germanium crystal.

In the case of planar channeling, the expression for the averaged potential energy $U(z)$ of the crystal lattice can be represented in the form of the averaged sum of potential energies of individual planes periodically arranged parallel to one another (see Fig. 8). The z axis is directed perpendicular to the lattice planes. $U(z)$ is the potential averaged in the x, y plane. In case of a crystal, it is a periodic function of z:

$$U(z) = \sum \frac{1}{S} \int_S U_{\mathrm{at}}(\mathbf{r})\, \mathrm{d}x\, \mathrm{d}y . \tag{75}$$

Let us expand $U(z)$ into a series in g:

$$U(z) = \sum_{m=-N}^{m=+N} U_m \exp(\mathrm{i}mgz) \tag{76}$$

and look for a solution to the equation in the form of a series:

$$\psi_n(z) = \frac{1}{\sqrt{d_n}} \exp(\mathrm{i}k_x z) \sum_{m=-N}^{m=+N} C_m^n \exp(\mathrm{i}mgz) . \tag{77}$$

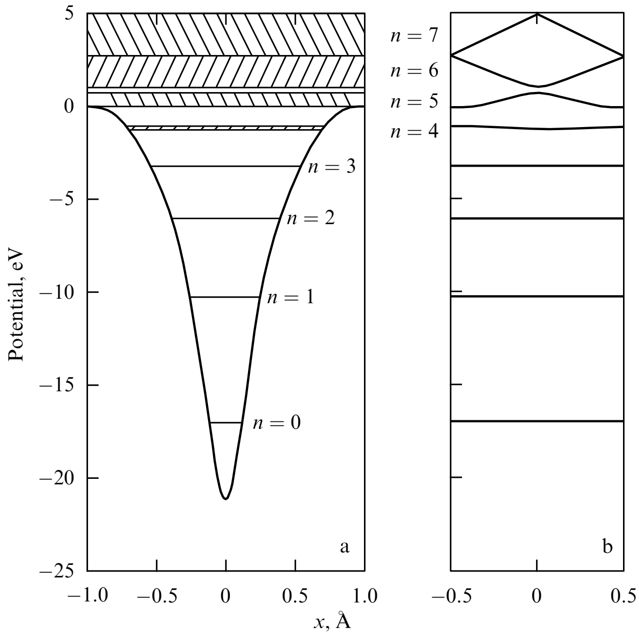

Figure 17. Transverse energy levels of 30.5 MeV electrons channeled in the (100) plane of a silicon crystal: (a) energy levels in a transverse potential well, (b) structure of energy bands mapped to the first Brillouin zone [124].

The Schrödinger equation for the transverse motion of a particle has the form

$$\left[-\frac{\hbar^2}{2\gamma m_0} \frac{\partial^2}{\partial^2 z} + U(z) \right] \psi(z) = E_\perp \psi(z) , \tag{78}$$

and is studied by a method analogous to that described above. By way of illustration, Fig. 17 presents the computed energy levels of channeled electrons in a silicon crystal [128a].

8.2 Channeling and radiative processes in crystals

Let us now consider a system of strings that form a crystal lattice. In this case, the transverse potential (63) corresponds to the averaged potential of the entire lattice. In other words, the summation in (63) should be done over the system of all strings periodically arranged in the crystal volume. The mathematical problem of the description of the charged particle motion becomes much more complicated. As noted above, it has been addressed in many original works and reviews [9, 10, 12, 27, 21, 23, 15, 28, 14, 16, 19]. Theoretical aspects of channeling in periodic media are summarized in a recent review by a group of theorists from Kharkov [31]. In what follows, we will follow the contents of their work (see also Refs [15, 19, 22, 23, 27, 28, 10]). Its second part is devoted to a comprehensive analysis of virtually all latest achievements in the field of interest, to which the authors themselves made an important contribution (see also Ref. [19] dealing with the passage of particles through a bent crystal, first considered in Ref. [19a], in view of controlling the trajectories of ultrarelativistic particles). Diverse mathematical methods are used (eikonal approximations, quasi-classical and Born approximations, the theory of multiple scattering, and statistical analysis). Also considered in the review are channeling processes; over-barrier, finite, and chaotic motion; multiple scattering, etc. These problems are viewed against a broad historical background.

With this in mind, we will confine ourselves to a brief review of the principal results, without going into detail in these problems.

It is evident that a positive particle with a transverse energy below the height of the potential barrier in the transverse potential (71) lies at one of the discrete energy levels of the potential well. Such a state is called finite motion. In the opposite case, the particle travels along the crystal, i.e. its motion is infinite. A negative particle can be in finite motion only if it enters the crystal at an angle $\theta < \theta_L$. Negative particles approach the crystal lattice closer than positive ones because the latter undergo Coulomb repulsion. This explains why various secondary reactions of negative particles with the lattice nuclei and atoms are more pronounced. The knowledge of these processes opens new prospects for spectroscopic studies of solids [15]. Also considered in the review is the theory of multiple scattering taking into account orientation effects and channeling in three-dimensional crystals. Various mathematical models based on statistical methods are used to analyse the chaotic motion of particles in crystalline media. Naturally, further theoretical studies and experiments are needed to promote the applicability of these complicated mathematical problems.

Of special importance for solid-state studies are processes of radiation by channeled particles observable during transitions between discrete energy levels, the characteristics of which depend on the parameters of the crystal lattice. Transverse energy levels usually lie in the optical range. However, the radiative-transition energy is shifted to the kiloelectronvolt region because Eqns (62), (74), (78) contain relativistic mass. The radiation is normally calculated using the dipole approximation, but its limits have to be exceeded as the energy of an emitting particle increases [133].

It turned out that the emission spectra of low-energy particles contain information about various crystal characteristics, such as the amplitude of thermal fluctuations, the form factor of lattice atoms, the density of defects, the isotopic composition, etc. This problem has been given a detailed consideration in reviews [15] and a monograph by V A Bazylev and N V Zhevago [28]. It is also worthwhile to mention a series of works on the effect of longitudinal ultrasound waves on radiation by channeled electrons presented at the last RREPS-99 Conference [90, pp. 14, 28, 64].

Starting from the first studies [8], much attention has been given to CR in a large number of original works referred to in later books and reviews [27, 28, 15, 128].

In conclusion, it should be emphasized that, although CR studies are a promising tool for characterizing the properties of solids, the experiments are difficult to conduct because of a variety of concomitant competing processes. Figure 18 from Ref. [129b] shows, on a logarithmic scale, the intensity spectra of Bethe – Heitler bremsstrahlung, CB (types A and B), DXR, and CR depending on the energy of a photon emitted by a particle with an energy of 30 MeV.

9. Theoretical problems of high-energy radiative electromagnetic processes

9.1 Introduction

It has been mentioned in Section 6 that a series of experiments carried out at CERN in the 1990s [101 – 103] brought about unexpected results at variance with the CB theory based on

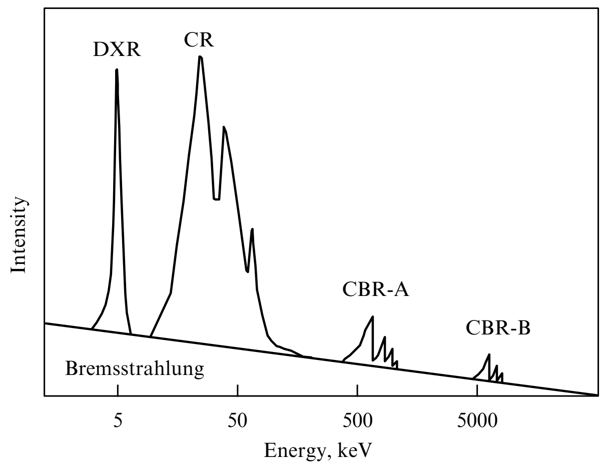

Figure 18. Intensity (on a logarithmic scale) of different radiation processes involving 20 MeV electrons depending on the energy of an emitted photon [126b].

the Born approximation, hence on the pseudophoton method. At first, these results did not yield to a simple physical interpretation. They were explained only after the studies published in Refs [30, 100 – 102]. It should be noted that the theoretical study [98] was preceded by works of Baryshevskiĭ and Tikhomirov [18, 23] and by the formulation of the Bayer – Katkov – Strakhovenko quasi-classical theory [17, 30], which predicted a variety of magnetic bremsstrahlung processes at ultrahigh energies.

Disregarding mathematical computation, we will try to present a physical interpretation of experiments [102, 103] based on the pseudophoton method and the work of Lindhard [98] concerning this problem. The Fermi – Weizsaecker – Williams method (see Section 5 and Fig. 6) implies that a resting electron experiences the action of the electric field (14) of a fast-moving atom and acquires a velocity perpendicular to the motion and equal to (we follow an example in Ref. [1, paragraph 2])

$$v_1 = \frac{2Ze^2}{mc\rho}\,, \tag{79}$$

where ρ is the impact parameter, which should be larger than the electron Compton length but smaller than the screening radius. It follows from (79) that the electron velocity remains low compared with the velocity of light even if the impact parameter is minimal, i.e. equal to the electron Compton wavelength. Based on the nonrelativistic classical radiation theory, it is easy to calculate the probability of long-wave photon emission with a frequency $\omega \ll 2c\gamma^2/\bar{\rho}$ in a laboratory frame of reference, where $\bar{\rho}$ is a certain average impact parameter. The formula thus obtained corresponds to the Bethe – Heitler cross section with a logarithmic precision. However, the radial electric field is not the sole factor that acts on a traveling recoil electron. It also experiences the effect of the magnetic field of a fast-moving atom perpendicular to the plane containing these electron and atom. In accordance with the classical theory, an electron influenced by a magnetic field across which it moves will emit quanta of magnetic bremsstrahlung [131]. However, the speed of the recoil electron being low, the magnetic bremsstrahlung emitted by the nonrelativistic electron will be weak in terms of both intensity and individual photon energy. This precludes the explanation of experimental results obtained at high energies.

The situation is changed dramatically if the electron motion in the field of a one-dimensional lattice (string) is considered taking into account channeling effects. It has been shown in Section 7.3 that orientation effects in the case of Coulomb scattering in a one-dimensional crystal may be apparent if the square of the Lindhard angle is much smaller than unity. In compliance with (61), the inverse square of the Lindhard angle determines the number of atoms in the string N_{coh} that coherently interact with the electron. Therefore, the electron is under the influence of N_{coh} coherently acting atoms, and its acquired transverse velocity $\mathbf{v}$ can approach the velocity of light. Evidently, for channeling to take place, the angle between the direction of electron velocity and the string axis must remain smaller than the Lindhard angle over the entire time of the process. In a magnetic bremsstrahlung event resulting in the emission of a photon with an energy close to that of the emitting electron (which remains relativistic after the emission), the angle of rotation of the electron velocity direction at the section of the trajectory where magnetic bremsstrahlung is produced will be typical of radiative processes, i.e. of the order of mc^2/E [130, Section 90]. It must be smaller than the Lindhard angle to ensure that the channeling process remain undisturbed. This is possible only if the radiating particle has an energy of the order of $m^2c^4/U \approx 100$ GeV. In such a case, magnetic bremsstrahlung has a quite different character (see Section 9.3).

The theory of magnetic bremsstrahlung has a long history and continues to be developed, growing more complicated in the ultrarelativistic energy range, where quantum effects and channeling become especially significant.

9.2 Classical theory

In the classical region, the radiation spectrum is built up of different harmonics with frequencies $\omega = q\omega_H$, where q is an integer and ω_H is the rotation frequency in a magnetic field (81). For an ultrarelativistic particle, the spectrum is quasi-continuous with a maximum at frequencies [131]

$$\omega_{\max} = q_{\max}\omega_H = \omega_H\left(\frac{E}{mc^2}\right)^3 = \frac{eH}{mc}\left(\frac{E}{mc^2}\right)^2 , \tag{80}$$

where

$$\omega_H = \frac{v}{r} = \frac{veH}{pc} = \frac{eH}{mc}\sqrt{1-\beta^2} \tag{81}$$

is the frequency of electron revolution in a plane perpendicular to the vector H, and r is the radius of the electron circular orbit in the same plane. If the particle travels in a plane lying at a small angle α to that normal to H, H in (80), (81) must be substituted by $H\cos\alpha$. Radiation by an ultrarelativistic electron is concentrated in the plane containing the recoil electron and the atom in motion, within an angle of order γ. The radiation intensity for the qth harmonic [131] is

$$I_q = \frac{2e^4H^2}{m^2c^2v}\left(1-\frac{v^2}{c^2}\right) \times\left[q\,\frac{v^2}{c^2}\,J'_{2q}\left(\frac{2qv}{c}\right) - q^2\left(1-\frac{v^2}{c^2}\right)\int_0^{v/c} J_{2q}(2q\xi)\,\mathrm{d}\xi\right]. \tag{82}$$

In an ultrarelativistic case, the formula for large q assumes the form

$$I_q = \frac{2e^4H^2}{\sqrt{\pi}\,m^2c^3}\,\frac{mc^2}{E}\,\sqrt{u}\left[-\Phi'(u) - \frac{u}{2}\int_u^{\infty}\Phi(u)\,\mathrm{d}u\right], \tag{83}$$

where

$$u = q^{2/3}\left(\frac{mc^2}{E}\right)^2 \tag{84}$$

and Φ is the Airy function.

Expressions (82)–(84) ought to be modified so as to take into account the longitudinal density effect which significantly alters both the spectrum and the intensity of emission of soft quanta. For synchronous radiation, this problem was solved in Ref. [132] and included by way of example in Ref. [1, Section 15]. It turned out that the above results remain valid for emitted photons in the frequency range

$$\omega_H\left(\frac{\omega_0}{\omega_H}\right)^{3/2} \leqslant \omega \leqslant \frac{\omega_H}{(1-\beta^2)^{3/2}} , \tag{85}$$

where ω_0 is the plasma frequency (10).

This restricts the magnetic field H by the condition

$$H \gg \frac{\omega_0 mc}{e}\sqrt{1-\beta^2} . \tag{86}$$

Beyond this range, that is if the inequality

$$\omega \ll \omega_H\left(\frac{\omega_0}{\omega_H}\right)^{3/2} \tag{87}$$

or

$$\omega \gg \frac{\omega_H}{(1-\beta^2)^{3/2}} , \tag{88}$$

is fulfilled, formula (83) acquires the following form [132]:

$$I_q = \frac{e^4H^2q^{1/2}}{2\sqrt{\pi}\,m^2c^3}\left(1-\frac{v^2}{c^2}\right)\left(1-\frac{v^2}{c^2}\,\varepsilon\right)^{1/4} \times\exp\left[-\frac{2}{3}\,q\left(1-\frac{v^2}{c^2}\,\varepsilon\right)^{3/2}\right]. \tag{89}$$

Thus, the intensity is strongly dependent on the dielectric constant of the medium.

9.3 Constant field approximation

The quantum theory of synchrotron radiation has been developed in numerous publications which demonstrated the important role of the parameter

$$\chi \approx \frac{\hbar\omega_H}{E}\left(\frac{E}{mc^2}\right)^3 \approx \frac{H}{H_0}\,\frac{E}{mc^2} . \tag{90}$$

Here, H_0 is the characteristic magnetic field:

$$H_0 = \frac{m^2c^3}{|e|\hbar} = 4.4\times10^{13}\ \text{G} . \tag{91}$$

At $\chi \ll 1$, the classical theory set forth above remains valid. In this case, the energy of an emitted photon is significantly smaller than the energy of the radiating particle, and the quantum recoil can be neglected. If $\chi \geqslant 1$,

$$\hbar\omega \sim E \tag{92}$$

and the electron energy E' after the emission event is much lower than the initial one:

$$E' \sim mc^2 \frac{H_0}{H} \ll E\,. \tag{93}$$

In this situation, taking into consideration quantum recoil leads to serious changes in formulas (82), (83). In quantum calculations, it is necessary to take into account the quantum properties of electron motion, except the recoil effect. However, if the condition

$$\frac{\hbar\omega_H}{E} = \frac{H}{H_0}\left(\frac{mc^2}{E}\right)^2 \ll 1\,, \tag{94}$$

is fulfilled, electrons are in quasi-classical motion and quasi-classical wave functions can be used for calculations [134, 137]. The first quantum corrections to the classical expressions were obtained in Refs [136, 137] and the quantum effects were fully taken into account in Ref. [135]. The final expressions for the intensity of magnetic bremsstrahlung in the ultrarelativistic limit have the form [138]

$$\frac{\mathrm{d}I}{\mathrm{d}\omega} = -\frac{e^2 m^2 \omega}{\sqrt{\pi}\,E^2}\left[\int_z^{\infty} \Phi(\xi)\,\mathrm{d}\xi + \left(\frac{2}{z} + \frac{\hbar\omega}{E}\,\chi z^{1/2}\right)\Phi'(z)\right], \tag{95}$$

$$z = \left(\frac{\hbar\omega}{E'\chi}\right)^{2/3} = \frac{m^2c^4}{E^2}\left(\frac{E\omega}{E'\omega_H}\right)^{2/3}, \tag{96}$$

where Φ is the Airy function.

Expressions (95), (96) and their relation to the corresponding classical formulas, depending on the parameter χ, are presented in a graphic form in Ref. [130, Section 90]. It follows that the probability of magnetic bremsstrahlung at $\chi > 1$ in a quantum case is significantly smaller than in the classical limit.

However, it increases substantially due to the coherent interaction of an electron with lattice atoms located within a coherence length. This fact permitted the authors of Refs [17, 30] to formulate a quasi-classical theory consistent with experimental findings.

Theoretical aspects of polarization phenomena and quantum electrodynamic effects associated with the production of electron – positron pairs were developed in Refs [18, 23]. Also, the authors of Refs [18, 23] comprehensively discussed these problems in application to interactions with periodic media and thus made an important contribution to this field of research.

An alternative approach to the same issue was employed in Refs [15, 28]. Of special interest are the theoretical results presented in Refs [15, 28] and their comparison with experimental findings in spectroscopy of solids obtained in channeling studies.

The effect of medium polarization on soft-photon magnetic bremsstrahlung in the quantum limit remains to be elucidated.

Ref. [27] compares undulating [139, 140] and synchrotron radiation with channeling radiation. For undulating radiation, the equation governing the motion of an emitting particle looks like (64) with the sole exception that its right-hand side contains an external driving force.

10. Conclusions

To conclude, I would like to emphasize that many problems touched upon in this review need further in-depth consideration. In the near future, we will witness new developments in these areas. I hope to address analogous issues in the next publication concerning radiative processes in amorphous media. I will therefore appreciate criticism from specialists in the field and their comments on the flaws and omissions in the present publication.

I am grateful to a large group of physicists for their help and encouragement during the preparation of this review. Special thanks are due to Darbinyan, Avakyan, and Ispiryan (Physical Institute, Yerevan); Artru (University of Lyon), Kottaus and Weiman (W Heisenberg Institute, Munich), Fiorito (Catholc University, Washington), Shul'ga and Shchagin (Physical-Technical Institute, Kharkov), Potylitsyn and Pivovarov (Institute of Nuclear Physics, Tomsk), Baryshevskiĭ (University of Minsk), Nasonov (University of Belgorod), Richter and Morokhovskii (Institute of Nuclear Physics, Darmstadt), Endo and Chufani (University of Hiroshima), Uggerhøj and Mikkelsen (Danish Institute, Arhus), Bake (Mainz), Nitta (University of Tokyo), Bayer, Katkov and Strakhovenko (Institute of Nuclear Physics, Novosibirsk), Zhevago and Kononets (Russian Research Center 'Kurchatov Institute', Moscow) who familiarized me with the current state of research on radiative processes and commented on different problems highlighted in the review. I am grateful to V Nikogosyan for assistance with the preparation of the manuscript. I am indebted to S Darbinyan for his careful reading of the manuscript and useful comments which I used in the final version of the review. This work was done in the framework of project 96-772 of the Armenian Ministry of Higher Education and Science and supported by INTAS grant 99-392.

References

1. Ter-Mikhaelyan M L *Vliyanie Sredy na Elektromagnitnye Protsessy pri Vysokikh Energiyakh* (High-Energy Electromagnetic Processes in Condensed Media) (Yerevan: Izd-vo Akad. Nauk Arm.SSR, 1969) [Translated into English (New York: Wiley-Interscience, 1972)]
2. Ginzburg V L *Prog. Opt.* XXXII, V, (1995); Ginzburg V L *Usp. Fiz. Nauk* **166** 1033 (1996) [*Phys. Usp.* **39** 973 (1996)]; Ginzburg V L *O Nauke, o Sebe i o Drugikh* (On Science, Myself, and Others) (Moscow: Nauka, 1997)
3. Feĭnberg E L *Priroda* (1) 30 (1994); Feĭnberg E L "Landau i drugie" ("Landau and others"), in *Vospominaniya o L D Landau* (Reminiscences of L D Landau) (Ed I M Khalatnikov) (Moscow: Nauka, 1988) p. 243
4. Berestetskiĭ V B, Lifshitz E M, Pitaevskiĭ L P *Kvantovaya Elektrodinamika* (Quantum Electrodynamics) (Moscow: Nauka, 1980) p. 452 (1989) p. 461 [Translated into English (Oxford: Pergamon Press, 1982)]
5. Feĭnberg E L *Usp. Fiz. Nauk* **58** 193 (1956); Feinberg E L, Pomerančuk I *Nuovo Cimento* (Suppl.) **3** 652 (1956)
6. Ter-Mikhhaelyan M L *Problemy Teoreticheskoĭ Fiziki* (Problems of Theoretical Physics) (Moscow: Nauka, 1972) p. 335; *Priroda* (12) 68 (1982)
7. Dremin I M *Mod. Phys. Lett. A* **13** 2789 (1998); Kaempfer B, Pavlenko O P *Phys. Lett. B* **477** 171 (2000)
8. Kumakhov M A *Phys. Lett. A* **57** 17 (1976); see [121]; Baryshevskiĭ V G, Dubovskaya I Ya *Dokl. Akad. Nauk SSSR* **231** 113 (1976); Baryshevskii V G, Dubovskaya I Ya *Phys. Status Solidi B* **82** 403 (1977); Andersen S K, Andersen and Augustyniak W M *Videns. Selsk. Mat. Fys. Med.* **39** 10 (1977); Bazylev V A, Zhevago N K *Zh. Eksp. Teor. Fiz.* **73** 1697 (1977) [*Sov. Phys. JETP* **46** 849 (1977)]; Terhune R W, Pantell R H *Appl. Phys. Lett.* **30** 265 (1977); Koptelov

E A, Kalashnikov N P, Preprint Inst. Yadern. Issled. Akad. Nauk SSSR No. 0054 (Moscow: Inst. Yadern. Issled., 1977); Akhiezer A I, Akhiezer I A, Shul'ga N F *Zh. Eksp. Teor. Fiz.* **76** 1244 (1979) [*Sov. Phys. JETP* **49** 625 (1979)]; Bayer V N, Katkov V M, Strakhovenko V M *Phys. Lett. A* **73** 414 (1979)

9. Lindhard J *Mat.-Fys. Medd. Dan. Vid. Selsk.* **34** (14) (1965) [Translated into Russian *Usp. Fiz. Nauk* **99** 249 (1969)]
10. (a) Thompson M W *Contemp. Phys.* **9** (4) 375 (1968) [Translated into Russian *Usp. Fiz. Nauk* **99** 297 (1969)]; Tulinov A F *Usp. Fiz. Nauk* **87** 585 (1965) [*Sov. Phys. Usp.* **8** 864 (1966)]; (b) Gemmell D S *Rev. Mod. Phys.* **46** 129 (1974)
11. Ryazanov M I *Usp. Fiz. Nauk* **114** 393 (1974) [*Sov. Phys. Usp.* **17** 815 (1974)]
12. Kumakhov M A *Usp. Fiz. Nauk* **127** 531 (1979) [*Sov. Phys. Usp.* **22** 177 (1979)]
13. Feĭnberg E L *Usp. Fiz. Nauk* **132** 255 (1980) [*Sov. Phys. Usp.* **23** 830 (1980)]; **58** 193 (1956); *Zh. Eksp. Teor. Fiz.* **50** 202 (1966) [*Sov. Phys. JETP* **23** 132 (1966)]; **29** 115 (1955) [*Sov. Phys. JETP* **2** 59 (1956)]; in *Shkola Molodykh Uchenykh po Fizike Vysokikh Energiĭ* (School on High-Energy Physics for Young Scientists) (Sukhumi, 5–16 October, 1972) (Materialy OIYaI, Vyp. P2-6867) (Dubna–Sukhumi: Izd. OIYaI, 1972) p. 56; Ritus V I *Problemy Teoreticheskoĭ Fiziki* (Problems of Theoretical Physics) (Moscow: Nauka, 1972) p. 248
14. Akhiezer A I, Shul'ga N F *Usp. Fiz. Nauk* **137** 561 (1982) [*Sov. Phys. Usp.* **25** 541 (1982)]
15. Bazylev V A, Zhevago N K *Usp. Fiz. Nauk* **137** 605 (1982) [*Sov. Phys. Usp.* **25** 565 (1982)]; **160** (12) 47 (1990) [*Sov. Phys. Usp.* **33** 1021 (1990)]
16. Akhiezer A I, Shul'ga N F *Usp. Fiz. Nauk* **151** 385 (1987) [*Sov. Phys. Usp.* **30** 129 (1987)]
17. Baĭer V N, Katkov V M, Strakhovenko V M *Usp. Fiz. Nauk* **159** 455 (1989) [*Sov. Phys. Usp.* **32** 972 (1989)]
18. Baryshevskiĭ V G, Tikhomirov V V *Usp. Fiz. Nauk* **159** 529 (1989) [*Sov. Phys. Usp.* **32** 1013 (1989)]
19. Akhiezer A I et al. *Usp. Fiz. Nauk* **165** 1165 (1995) [*Sov. Phys. Usp.* **38** 1119 (1995)]; (a) Tsyganov É N, Preprint Fermi-Lab No. 682 (1976); *Pis'ma Zh. Eksp. Teor. Fiz.* **26** 403 (1979) [*JETP Lett.* **26** 150 (1979)]
20. Baĭer V N, Katkov V M, Fadin V S *Izluchenie Relyativistskikh Elektronov* (Radiation by Relativistic Electrons) (Moscow: Atomizdat, 1973)
21. Kalashnikov N P *Kogerentnye Vzaimodeĭstviya Zaryazhennykh Chastits v Monokristallakh* (Coherent Interactions of Charged Particles in Single Crystals) (Moscow: Atomizdat, 1981) [Translated into English (Chur: Harwood Acad. Publ., 1988)]
22. Kalashnikov N P, Remizovich V S, Ryazanov M I *Stolknovenie Bystrykh Zaryazhennykh Chastits v Tverdykh Telakh* (Collisions of Fast Charged Particles in Solids) (Moscow: Atomizdat, 1980) [Translated into English (New York: Gordon and Breach, 1985)]
23. Baryshevskiĭ V G *Kanalirovanie, Izluchenie i Reaktsii v Kristallakh pri Vysokikh Energiyakh* (Channeling, Radiation and Reactions in Crystals at High Energies) (Minsk: Izd. BGU, 1982)
24. Garibyan G M, Yan Shi *Rentgenovskoe Perekhodnoe Izluchenie* (X-Ray Transition Radiation) (Yerevan: Izd. Akad. Nauk Arm SSR, 1983)
25. Ginzburg V L, Tsytovich V N *Perekhodnoe Izluchenie i Perekhodnoe Rasseyanie* (Transition Radiation and Transition Scattering) (Moscow: Nauka, 1984) [Translated into English (Bristol: A. Hilger, 1990)]
26. Ryazanov M I *Elektrodinamika Kondensirovannogo Veshchestva* (Condensed Matter Electrodynamics) (Moscow: Nauka, 1984)
27. Kumakhov M A *Izluchenie Kanalirovannykh Chastits v Kristallakh* (Radiation by Channeled Particles in Crystals) (Moscow: Energoatomizdat, 1986); Kumakhov M A, Shirmer G *Atomnye Stolknoveniya v Kristallakh* (Atomic Collisions in Crystals) (Moscow: Atomizdat, 1980) [Translated into English (New York: Gordon and Breach, 1989)]
28. Bazylev V A, Zhevago N K *Izluchenie Bystrykh Chastits v Veshchestve i vo Vneshnikh Polyakh* (Radiation by Fast Particles in Matter and External Fields) (Moscow: Nauka, 1987)
29. Potylitsyn A P *Polyarizovannye Fotonnye Puchki Vysokoĭ Energii* (High Energy Polarized Photon Beams) (Moscow: Energoatomizdat, 1987)
30. Baier V N, Katkov V M, Strakhovenko V M *Elektromagnitnye Protsessy pri Vysokoĭ Energii v Orientirovannykh Monokrystallakh* (Electromagnetic Processes at High Energies in Oriented Single Crystals) (Novosibirsk: Nauka, 1989) [Translated into English (Singapore: World Scientific, 1998)]
31. Akhiezer A I, Shul'ga N F *Elektrodinamika Vysokikh Energiĭ v Veshchestve* (High-Energy Electrodynamics in Matter) (Moscow: Nauka, 1993) [Translated into English (Luxemburg: Gordon and Breach, 1996)]; Akhiezer A I, Shulga N F, Truten V I "Coherent effects in scattering and radiation of high-energy particles in crystals", in *Physics Reviews* Vol. 19 (Ed. I M Khalatnikov) (Chur: Harwood Acad. Publ., 1998)
32. Vorob'ev S A et al. *Pis'ma Zh. Eksp. Teor. Fiz.* **41** 3 (1985) [*JETP Lett.* **41** 1 (1985)]
33. Adishchev Yu N et al. *Pis'ma Zh. Eksp. Teor. Fiz.* **41** 295 (1985) [*JETP Lett.* **41** 361 (1985)]; *Zh. Eksp. Teor. Fiz.* **90** 829 (1986) [*Sov. Phys. JETP* **63** 488 (1986)]
34. Avakyan R O et al. *Pis'ma Zh. Eksp. Teor. Fiz.* **45** 313 (1987) [*JETP Lett.* **45** 396 (1987)]
35. Shchagin A V, Pristupa V I, Khizhnyak N A *Phys. Lett. A* **148** 485 (1990); *Nucl. Instrum. Methods B* **99** 277 (1995); Shchagin A V, Khizhnyak N A *Nucl. Instrum. Methods B* **119** 115 (1996)
36. Afanasenko V P et al. *Phys. Lett. A* **170** 315 (1992)
37. Asano S et al. *Phys. Rev. Lett.* **70** 3247 (1993)
38. Fiorito R B et al. *Phys. Rev. Lett.* **71** 704 (1993)
39. Shchagin A V, Pristupa V I, Khizhnyak N A, in *Proc. of RREPS* (Tomsk, Russia, 1993) p. 62; *Nucl. Instrum. Methods B* **99** 277 (1995); **119** 115 (1996)
40. Nitta H *Phys. Rev. B* **45** 7621 (1992); *Phys. Lett. A* **158** 270 (1991); *Nucl. Instrum. Methods B* **115** 401 (1996)
41. Freudenberger J et al. *Nucl. Instrum. Methods B* **115** 408 (1996)
42. Freudenberger J et al. *Appl. Phys. Lett.* **70** 267 (1997)
43. Brenzinger K-H et al. *Phys. Rev. Lett.* **79** 2462 (1997); *Z. Phys. A* **358** 107 (1997)
44. Doerk Th et al., in *Intern. Workshop* (Tabarz, Germany, 9–12 June, 1998) Abstract
45. Morokhovskii V V et al. *Phys. Rev. Lett.* **79** 4389 (1997); Morokhovskii V V, Dissertation D17 (Darmstadt: Technische Universitaet Darmstadt, 1998)
46. Schmidt K H et al. *Nucl. Instrum. Methods B* **145** 8 (1998); Morokhovskii V V et al. *Nucl. Instrum. Methods B* **145** 14 (1998)
47. Kottaus R et al. *Proc. SPIE* **3443** 105 (1998)
48. Shchagin A V *Phys. Lett. A* **247** 27 (1998)
49. Ter-Mikhaelyan M L *Dokl. Akad. Nauk SSSR* **94** 1033 (1954)
50. Adishchev Yu N et al. *Pis'ma Zh. Eksp. Teor. Fiz.* **48** 311 (1988) [*JETP Lett.* **48** 342 (1988)]; Adishchev Yu N et al. *Nucl. Instrum. Methods B* **44** 130 (1989)
51. Endo I et al. *Phys. Rev. E* **51** 6305 (1995)
52. Fiorito R B et al. *Phys. Rev. E* **51** R2759 (1995)
53. Freudenberger J et al. *Phys. Rev. Lett.* **74** 2487 (1995)
54. Feranchuk I D, Ivashin A V *J. Phys.* (Paris) **46** 1981 (1985)
55. Amosov K Yu et al. *Phys. Rev. E* **47** 2207 (1993)
56. Avakian R O et al. *Rad. Effects Defects Solids* **117** 17 (1991); Aslanyan H A, Mkrtchyan A H, in *Intern. Workshop* (Tabarz, Germany, 9–12 June, 1998) Abstract; Mkrtchyan A R et al. *Phys. Lett. A* **152** 297 (1991)
57. Fiorito R B et al. *Nucl. Instrum. Methods B* **79** 758 (1993)
58. Garibyan G M *Zh. Eksp. Teor. Fiz.* **37** 527 (1959) [*Sov. Phys. JETP* **10** 372 (1960)]
59. Barsukov K A *Zh. Eksp. Teor. Fiz.* **37** 1106 (1959) [*Sov. Phys. JETP* **10** 787 (1960)]
60. Frank I M *Usp. Fiz. Nauk* **75** 231 (1961) [*Sov. Phys. Usp.* **4** 740 (1962)]
61. Ter-Mikhaelyan M L *Dokl. Akad. Nauk SSSR* **134** 318 (1960)
62. Ter-Mikaelyan M L *Nucl. Phys.* **24** 43 (1961); Ter-Mikhaelyan M L *Pis'ma Zh. Eksp. Teor. Fiz.* **8** 100 (1968) [*JETP Lett.* **8** 59 (1968)]; Ter-Mikhaelyan M L, Gazazyan A D *Zh. Eksp. Teor. Fiz.* **39** 1693 (1960) [*Sov. Phys. JETP* **12** 494 (1961)]
63. Arutyunyan F R, Ispiryan K A, Oganesyan A G *Yad. Fiz.* **1** 842 (1965)
64. Arutyunyan F R, Ter-Mikhaelyan M L *Usp. Fiz. Nauk* **107** 332 (1972) [*Sov. Phys. Usp.* **15** 102 (1972)]
65. Ginzburg V L *Priroda* (8) 56 (1975); Ginzburg V L, Tsytovich V N *Phys. Rep.* **49** 1 (1979)
66. Cherry M L, Hartmann G *Phys. Rev. D* **10** 3594 (1974)
67. Artru X, Yodh G B, Mennessier G *Phys. Rev. D* **12** 1289 (1975)

68. Deutschmann M et al. *Nucl. Instrum. Methods B* **180** 409 (1981); Fabjan C W, Struczinski W *Phys. Lett. B* **57** 483 (1975)
69. Dolgoshein B *Nucl. Instrum. Methods A* **326** 434 (1993)
70. Ebert P J et al. *Phys. Rev. Lett.* **54** 893 (1985)
71. Piestrup M A et al. *Phys. Rev. A* **32** 917 (1985)
72. Piestrup M A et al. *Appl. Phys. Lett.* **58** 2692 (1991); **59** 189 (1991)
73. Moran M J et al. *Phys. Rev. Lett.* **57** 1223 (1986)
74. Goedtkindt P et al. *Nucl. Instrum. Methods B* **56 – 57** 1060 (1991)
75. Goedtkindt P et al. *Microelectron. Eng.* **13** 327 (1991)
76. Piestrup M A et al. *Phys. Rev. A* **45** 1183 (1992)
77. Tanaka T et al. *Nucl. Instrum. Methods B* **93** 21 (1994)
78. Awata T et al. *Radiat. Phys. Chem.* **50** (3) 207 (1997); Awata T et al., in *Application of Accelerator in Research and Industry* (Eds J L Duggan, I I Morgan) (New-York: AIP, 1997); *Beam Sci. Technol.* **3** 10 (1998)
79. Yamada K, Hosokawa T, Takenaka H *Phys. Rev. A* **59** 3673 (1999)
80. Asano S et al. *Phys. Rev. Lett.* **70** 3247 (1993)
81. Kaplan A E, Law C T, Shkolnikov P L *Phys. Rev. E* **52** 6795 (1995)
82. Potylitsyn A P, Verzilov V A *Phys. Lett. A* **209** 380 (1995)
83. Andreyashkin M Yu et al. *Nucl. Instrum. Methods B* **119** 108 (1996); Andreyashkin M Yu et al. *Pis'ma Zh. Eksp. Teor. Fiz* **65** 594 (1997) [*JETP Lett.* **65** 625 (1997)]
84. Takashima Y, Aramitsu K, Endo I *Nucl. Instrum. Methods B* **145** 25 (1998)
85. Potylitsyn A P *Phys. Lett. A* **238** 112 (1998)
86. Potylitsyn A P *Nucl. Instrum. Methods B* **145** 60 (1998)
87. Baryshevsky V G *Nucl. Instrum. Methods B* **122** 13 (1997)
88. Artru X, Rullhusen P *Nucl. Instrum. Methods B* **145** 1 (1998)
89. Nasonov N *Phys. Lett. A* **246** 148 (1998)
90. *Nucl. Instrum. Methods B* **145**; *Beam Interaction with Materials&Atoms* (Eds S K Andersen, L E Rehn) (Amsterdam: Elsevier, 1998); *IV Intern. Symp. RREPS, Russia, Lake Baikal, 1999,* Abstracts
91. *4 Intern. Workshop on Radiation Physics with Relativistic Electrons* (Eds H Backe, W Lauth, T Walcher) (Tabarz, Germany, 1998) Abstracts
92. (a) Avakyan R, in *Trudy Mezhdunarodnoĭ Konferentsii po Apparature i Fizike Vysokikh Energiĭ* Vol. 3 (Proc. of Intern. Conf. on High-Energy Instrumentation and Physics) (Dubna: OIYaI, 1970) p. 746; (b) Toboiyama M et al. *Phys. Rev. B* **44** 9248 (1991); *Phys. Lett. A* **166** 140 (1992)
93. (a) Avakian R O et al. *Rad. Eff. Defect Solids* **117** 33 (1991); Darbinyan S M, Ispiryan K A, Margaryan A T *Izv. Akad. Nauk Arm. SSR Ser. Fiz.* **23** (4) 177 (1988) [*Sov. J. Contemp. Phys.* **23** (4) 1 (1988)]; Potylitsyn A P *Pis'ma Zh. Eksp. Teor. Fiz.* **53** 12 (1991) [*JETP Lett.* **53** 12 (1991)];
(b) Sáenz A W, Überall H *Phys. Rev. B* **25** 4418 (1982); Kimball J C, Cue N *Phys. Rev. Lett.* **57** 1935 (1986); Cue N, Kimball J C *Phys. Lett. A* **124** 191 (1987)
94. Walker R L et al. *Phys. Rev. Lett.* **25** 5 (1970); Walker R L, Berman B L, Bloom S D *Phys. Rev. A* **11** 736 (1975); Morokhovskiĭ V L et al. *Pis'ma Zh. Eksp. Teor. Fiz.* **16** 162 (1972) [*JETP Lett.* **16** 108 (1972)]; Vorobiev A A, Kaplin V V, Vorobiev S A *Nucl. Instrum. Methods* **127** 265 (1975)
95. (a) Avakyan R O et al. *Zh. Eksp. Teor. Fiz.* **82** 1825 (1982) [*Sov. Phys. JETP* **55** 915 (1982)]; Avakyan R O et al. *Rad. Eff.* **91** 257 (1986);
(b) Belkacem A et al. *Phys. Lett. B* **177** 211 (1986)
96. Uggerhøi E "Channeling and related phenomena for Gev particles", in *Relativistic Channeling* (Eds R A Carrigan, J A Ellison) (New York: Plenum Press, 1987)
97. (a) Kimball J C, Cue N *Phys. Rep.* **125** 69 (1985); Baryshevskiĭ V G, Tikhomirov V V *Zh. Eksp. Teor. Fiz.* **85** 232 (1983) [*Sov. Phys. JETP* **58** 135 (1983)]; Baier V N, Katkov V M, Strakhovenko V M *Nucl. Instrum. Methods B* **16** 5 (1986);
(b) Belkacem A, Cue N, Kimball J C *Phys. Lett. A* **111** 86 (1985)
98. Lindhard J *Phys. Rev. A* **43** 6032 (1991)
99. Sorensen A H, Uggerhøj E *Nucl. Sci. Appl. A* **3** 147 (1989); Medenwaldt R et al. *Phys. Rev. Lett.* **63** 2827 (1989); *Phys. Lett. B* **242** 517 (1990)
100. Kononets Yu V, Tupitsyn I S *Pis'ma Zh. Eksp. Teor. Fiz.* **59** 491 (1994) [*JETP Lett.* **59** 516 (1994)]; *Pis'ma Zh. Eksp. Teor. Fiz.* **57** 148 (1993) [*JETP Lett.* **57** 151 (1993)]
101. Darbinyan S M, Ter-Isaakyan N L *Pis'ma Zh. Eksp. Teor. Fiz.* **69** 171 (1999) [*JETP Lett.* **69** 180 (1999)]
102. Medenwaldt R et al., CERN-PRE/92-21 (10 Feb. 1992); *Phys. Lett. B* **281** 153 (1992)
103. Vilakazi Z Z et al. (see in [92])
104. Belkacem A et al. *Phys. Rev. Lett.* **58** 1196 (1987)
105. Kirzebom K et al. *Phys. Lett. B* **439** 347 (1999)
106. Adishchev Yu N et al. *Pis'ma Zh. Eksp. Teor. Fiz.* **33** 478 (1981) [*JETP Lett.* **33** 462 (1981)]
107. Bilokon H et al. *Nucl. Instrum. Methods* **204** 299 (1983); Bussey P J et al. *Nucl. Instrum. Methods* **211** 301 (1983)
108. Yoshida K et al. *Phys. Rev. Lett.* **80** 1437 (1998)
109. Artru X et al. *Nucl. Instrum. Methods B* **119** 246 (1996)
110. Endo I et al. *Phys. Lett. A* **164** 319 (1992)
111. Endo I et al. *Phys. Lett. A* **146** 150 (1990)
112. Artru X (a) *Phys. Lett. A* **128** 302 (1988); (b) *Phys. Lett. B* **313** 483 (1993); Baurichter A et al. *Phys. Rev. Lett.* **79** 3415 (1997)
113. Lindhard J, Dan K *Videsk. Selsk. Mat. Fys. Medd.* **34** 14 (1965); *Phys. Lett.* **12** 126 (1964)
114. Uggerhøj E *Phys. Lett.* **22** 382 (1966)
115. Alguard M J et al. *Phys. Rev. Lett.* **42** 1148 (1979); Swent R L et al. *Phys. Rev. Lett.* **43** 1723 (1979); Agan'yants A O et al. *Pis'ma Zh. Eksp. Teor. Fiz.* **29** 554 (1979) [*JETP Lett.* **29** 505 (1979)]
116. Kumakhov M A, Wedell R *Radiat. Eff.* **22** 14 (1975)
117. Andersen J U, Eriksen K R, Laegsgaard E *Phys. Scripta* **24** 588 (1981); Andersen J U, Laegsgaard E *Nucl. Instrum. Methods B* **33** 11 (1988)
118. Freudenberger J et al. *Nucl. Instrum. Methods B* **119** 123 (1996)
119. (a) Morokhovskyi V V et al. *Phys. Rev. B* **61** 3347 (2000);
(b) Blazhevich S V et al. *Phys. Lett. A* **195** 210 (1994)
120. Genz H et al. *Phys. Rev. B* **53** 8922 (1996)
121. Kumakhov M A *Phys. Status Solidi B* **84** 41 (1977)
122. Rzepka M et al. *Phys. Rev. B* **52** 771 (1995)
123. Rzepka M et al. *Nucl. Instrum. Methods B* **90** 186 (1994)
124. Chouffani K et al. *Nucl. Instrum. Methods B* **152** 479 (1999)
125. Adischev Y et al. *Radiat. Eff.* **91** 247 (1986)
126. (a) Weinmann P M et al. *Nucl. Instrum. Methods B* **145** 113 (1998); Weinmann P M, Dissertation, M.P.I.-PhE-98-07 (Münich, 1998); (b) Überall H et al. *Proc. SPIE* **1552** 198 (1991)
127. Buschhorn G et al. *Phys. Rev. B* **55** 6196 (1996)
128. Saenz A W, Überall W (Eds) *Coherent Radiation Sources* (Berlin: Springer-Verlag,1985); Ohtsuki Y-H *Charged Beam Interaction with Solids* (London: Taylor & Francis Ltd, 1983) [Translated into Russian (Moscow: Mir, 1985)]; Ognev L I *Usp. Fiz. Nauk* **154** 691 (1988) [*Sov. Phys. Usp.* **31** 372 (1988)]; Ryabov V A *Effekt Kanalirovaniya* (Channalling Effect) (Moscow: Energoatomizdat, 1994); Rullhusen P, Artru X, Dhez P, in *Synchrotron Radiation Techniques* Vol. 4 (Singapore: World Scientific, 1998);
(a) Chouffani K, Überall H *Phys. Status Solidi B* **213** 107 (1999)
129. Ter-Mikhaelyan M L *Zh. Eksp. Teor. Fiz.* **25** 289 (1953); Thesis of Candidate's Phys. Mat. Sci. (Moscow: Fiz. Inst. Akad. Nauk, 1953)
130. Berestetskiĭ V B, Lifshitz E M, Pitaevskiĭ L P *Kvantovaya Elektrodinamika* (Quantum Electrodynamics) (Moscow: Nauka, 1989) [Translated into English (Oxford: Pergamon Press, 1982)]
131. Landau L D, Lifshitz E M *Teoriya Polya* (The Classical Theory of Fields) (Moscow: Nauka, 1967) [Translated into English (Oxford: Pergamon Press, 1971)]; Schott G A *Electromagnetic Radiation and the Mechanical Reactions Arising from It* (Cambridge: Univ. Press, 1912)
132. Ter-Mikhaelyan M L *Izv. Akad. Nauk Arm. SSR Ser. Fiz. Mat. Nauk* **12** (3) 95 (1950)
133. Kumakhov M A, Trikalinos Kh G *Zh. Eksp. Teor. Fiz.* **78** 1623 (1980) [*Sov. Phys. JETP* **51** 828 (1980)]; Kumakhov M A, Trikalinos Ch G *Phys. Status Solidi B* **99** 449 (1980); Bazylev V A, Glebov V I, Zhevago N K *Zh. Eksp. Teor. Fiz.* **78** 62 (1980) [*Sov. Phys. JETP* **51** 7 (1980)]
134. Baĭer V N, Katkov V M *Zh. Eksp. Teor. Fiz.* **53** 1478 (1967) [*Sov. Phys. JETP* **26** 854 (1967)]
135. Klepikov N P *Zh. Eksp. Teor. Fiz.* **26** 19 (1954)
136. Sokolov A A, Klepikov N P, Ternov I M *Zh. Eksp. Teor. Fiz.* **23** 632 (1952)
137. Schwinger J *Proc. Natl. Acad. Sci. USA* **40** 132 (1954)
138. Nikishov A I, Ritus V I *Tr. Fiz. Inst. Akad. Nauk SSSR* **111** 3 (Moscow: Nauka, 1979)
139. Ginzburg V L *Izv. Akad. Nauk SSSR Ser. Fiz.* **11** 165 (1947)
140. Korkhmazyan N A *Izv. Akad. Nauk Arm. SSR Ser. Fiz.* **7** 144 (1972)